Master's Thesis

Amplitude Level Evolution in QCD

A dissertation submitted to the University of Manchester

for the degree of Master of Science by Research in

The Faculty of Science and Engineering

2019

Robert J. Mears

Department of Physics and Astronomy

School of Natural Sciences

Contents

Word Count: 3247

List of Figures

List of Tables

Abstract

The Faculty of Science and Engineering

Department of Physics and Astronomy

Master of Science by Research

Amplitude Level Evolution in QCD

by Robert J. Mears

Predictions for non-global observables necessitate the resummation procedure to include real emissions as well as virtuals. The FKS algorithm is a colour basis independent method of recursively inserting real emissions whilst interweaving virtual corrections up to all orders. The algorithm has so far not be shown to be collinear safe to all orders, however, and must be regularised using a collinear cut-off λ. I use the FKS algorithm in the Colour flow basis to calculate the gaps-between-jets observable at first, second and third order. The first order calculation is shown to be analytically λ independent. The second and third order calculations are numerically shown to exhibit λ independence for $\lambda < 10^{-4}$ and $\lambda < 10^{-5}$ respectively.

Declaration of Authorship

I, Robert J. Mears, declare that this thesis titled, "Amplitude Level Evolution in QCD" and the work presented in it are my own. I confirm that:

- that no portion of the work referred to in the dissertation has been submitted in support of an application for another degree or qualification of this or any other university or other institute of learning. .

- Further information on the conditions under which disclosure, publication and commercialisation of this dissertation, the Copyright and any Intellectual Property and/or Reproductions described in it may take place is available in the University IP Policy ,in any relevant Dissertation restriction declarations deposited in the University Library, The University Librarys regulations and in The Universitys policy on Presentation of Dissertations

Acknowledgements

I wish to acknowledge the love and support received from my mother Caroline and father Rex. Thank you to my girlfriend Leah for her belief, encouragement and patience. Thank you to my brother George and sister Jess for always being there for me in stressful moments. Thank you to my friend Danny for his support and our lunch time conversations.

I wish to express my gratitude towards my supervisor Professor Jeffrey Forshaw for giving advice and support whenever it was needed. I also greatly appreciate being given the opportunity to contribute in some way to the research.

I also wish to thank my fellow QCD theorists: Matt De Angelis, Kiran Ostrolenk, Jack Helliwell, Jack Holguin and Baptiste Cabouat. I asked many questions over the course of the year and everyone was always willing to take time to answer them. Your collective company made the long days of frustration enjoyable and I look back on the year fondly.

"*Young man, in mathematics you don't understand things. You just get used to them.*"

John Von Neumann

Chapter 1

Introduction

1.1 Introduction

Quantum Chromodynamics (QCD) is the relativistic quantum field theory of strong interactions. It describes interactions between colour charged fields: quarks, anti-quarks and gluons, collectively known as partons. It is a $SU(3)c$ gauge theory meaning the quark fields, in the triplet representation, are invariant under the local gauge transformations generated by 3×3 matrices in the fundamental representation, the $8\,(= N^2 - 1)$ generators of the group. The 8 corresponding gauge fields are the gluon fields and the set of gluons is the octet representation of the group [1, 2, 3].

The Lagrangian for QCD, ignoring the ghost and gauge fixing terms, is

$$\mathcal{L} = -\frac{1}{4} F^a_{\mu\nu} F^{\mu\nu}_a + \sum_{flavours} \bar{q}_i \left(i \not{D} - m\right)_{ij} q_j \tag{1.1}$$

where m is the quark mass and the covariant derivative is given by

$$\not{D}_{ij} = \not{\partial} \delta_{ij} + i g \boldsymbol{t}^a_{ij} \not{A}^a \tag{1.2}$$

which transforms under local gauge transformations in the same way as the field it acts on. The gluon gauge fields A^a_μ act to absorb the residual derivative terms when the gauge fields are also transformed [1, 2, 3]. The field strength tensor is given by

$$\begin{aligned} F^a_{\mu\nu} &= \frac{1}{ig}[D_\mu, D_\nu] \\ &= \partial_\mu A^a_\nu - \partial_\nu A^a_\mu - g f^{abc} A^b_\mu A^c_\nu \end{aligned} \tag{1.3}$$

where g is the strong coupling constant and the group structure constants are defined in terms of the fundamental 3×3 matrices

$$if^{abc}\boldsymbol{t}^c_{ij} = [\boldsymbol{t}^a, \boldsymbol{t}^b]. \tag{1.4}$$

The structure constants themselves obey

$$\begin{aligned} if^{abc}\boldsymbol{T}^c &= [\boldsymbol{T}^a, \boldsymbol{T}^b] \\ (\boldsymbol{T}^a)_{bc} &= -if^{abc} \end{aligned} \tag{1.5}$$

where $(\boldsymbol{T}^a)_{bc}$ is a generator of the adjoint representation of $SU(3)_c$. These 8×8 matrices generate colour space transformations of the octet (gluon) representation. The $SU(3)_c$ group is non-abelian meaning the structure constants f^{abc} are non-zero. Inserting the field strength tensor into the Lagrangian leads to terms which correspond to triple and quartic gluon vertices: Gluons are colour charged and can therefore self interact. This is the major distinction between Quantum Electrodynamics and QCD which makes higher order calculations in QCD more challenging [4]. Any high multiplicity calculations must include the effects of gluons radiating from other gluons rather than just radiating from quarks.

At particle colliders high energy colour charged particles radiate via Bremsstrahlung and pair production to form a parton shower, a cascade of colour charged radiation. To test theory against experiment, properties of parton showers must be computed. Performing these calculations perturbatively using the full Feynman rules becomes impossible beyond a few orders as the work involved increases factorially with the order [1]. Whats more, the Feynman amplitudes are enhanced for certain regions of the phase space meaning fixed order calculations in perturbation theory lead to unreliable predictions for observables: there will always be terms from higher order diagrams that are more dominant but not being included [4]. For a particular Feynman graph there may be several enhanced regions but the nature of the observable being computed determines which are most significant. The approach taken is then to approximate the shower by considering the Feynman graphs only in the enhanced regions.

Gluons whose momentum components are all much smaller than the scale of its

parent parton are said to be soft gluons [5]. Each soft gluon provides an enhancement of

$$\int_{\mu}^{Q} \frac{dE_k}{E_k} = \ln\left(\frac{Q}{\mu}\right) \equiv L \tag{1.6}$$

where μ is an arbitrary 'soft' scale which must be allowed to tend to zero to include the possibility of infinitesimally soft gluon emissions. The upper scale Q is the hard scale and corresponds to the scale of the hard process being dressed with radiation. In this limit the Eikonal rules are valid which are a set of simplified Feynman rules [5]. These approximations lead to further simplifications in terms of the spinors and it can be shown (see chapter 2) that

$$d\sigma_{n+1} = d\sigma_n \frac{dE_k}{E_k} \frac{d\Omega_k}{2\pi} \frac{\alpha_s}{2\pi} \sum_{i,j} C_{ij} \frac{E_k^2 p_i \cdot p_j}{p_i \cdot k p_j \cdot k} \tag{1.7}$$

where: $d\sigma_{n+1}$ is the differential cross section for the process of interest plus one gluon; $d\sigma_n$ is the differential cross section for the original process;E_k and k are the energy and four-momentum of the soft gluon; $d\Omega_k$ is the differential solid angle of the soft gluon; p_i, p_j are the momenta of external legs from which the gluon was emitted in the amplitude and conjugate amplitude and C_{ij} is a colour factor calculated by taking the trace over the colour algebra [1]. This is the soft factorisation theorem and it states that the cross section for a hard process dressed with one soft real gluon can be factorised into the cross-section for the hard process and the probability of soft emission. This is the basis for all soft parton branching algorithms [6].

Factorisation of the emission process (described above) combined with factorisation of the phase space allows for the process to be exponentiated [7] and thus applied to all orders. This is the basis of all orders resummation. An example of soft gluon resummation for an observable that is inclusive above a cut off scale is [8]. The factorised result for the first soft gluon virtual correction is exponentiated to obtain a perturbative series in terms of $\alpha_s L$. This approach assumed real emissions were not required as they would be cancelled exactly against virtual contributions via the the Bloch-Nordsieck theorem. This states that for every real correction at the cross section level there is an equal and opposite contribution from a virtual correction, provided the observable is inclusive over the entire phase space. Diagrammatically it

corresponds to a sum over cuts of the cross section diagram with the cut representing where the amplitude ends and the conjugate amplitude begins [9].

This cancellation does not occur for non-global observables which are not inclusive of real emissions over the entire phase space. For example, the gaps between jets (GBJ) observable. The hard process $e^+e^- \to q\bar{q}$ produces a back to back quark-anti-quark pair in the centre of mass frame. GBJ vetoes emissions into the region between back to back jets. Because any detector has a finite resolution the theoretical prediction for the result must be inclusive of the entire angular region below some experimental energy cut-off ρ. These conditions are implemented in the calculation by appending a set of Heaviside step functions to the phase space integrals for real emissions. The measurement function for GBJ is

$$u(k) = \Theta_{out}(k) + \Theta_{in}\Theta(\rho > E_k) \tag{1.8}$$

where $\Theta_{out}(k)$ is unity if k is in the out of gap region and $\Theta_{in}\Theta(\rho > E_k)$ is unity if k is in the gap region and has energy below the experimental cut off [10]. Combining equation 1.8 with

$$\Theta_{out}(k) + \Theta_{in}(k) \;=\; 1 \tag{1.9}$$

gives the useful result

$$u(k) - 1 \;=\; -\Theta_{in}\Theta(\rho < E_k). \tag{1.10}$$

As pointed out in [11], observables of this type lead to corrections being enhanced by a non-global logarithm. For the matrix element squared A of a generic scattering event, the real and virtual corrections combine to give

$$\begin{aligned} R + V &= \int_\mu^Q \frac{dE_k}{E_k} \int_{all} d\Omega_k \, A \; (u(k) - 1) \\ &= -\int_\rho^Q \frac{dE_k}{E_k} \int_{in} d\Omega_k \, A \\ &= -\ln\left(\frac{Q}{\rho}\right) \int_{in} d\Omega_k \, A \end{aligned} \tag{1.11}$$

where $u(k)$ acts to select the phase space region defined for the real contribution (see above). The virtual correction's phase space is global but imaginary factors result in a relative minus sign. The second line follows from equation 1.10. The logarithmic

enhancement is not singular as ρ is defined to be the finite experimental cut-off but it is small enough for the non-global logarithm $\ln\left(\frac{Q}{\rho}\right)$ to provide significant enhancements. An arbitrary number of reals must therefore be included in the resummation procedure [11]. This is a significantly more difficult process than resumming the first order loop correction.

QCD becomes increasingly complicated with successive real emissions. The main reason for this is the non-abelian colour matrices which accompany every emission. Each gluon considered acts to complicate the colour structure further and the problem of calculating the trace over the long list of $SU(3)_c$ matrices quickly becomes intractable. Historically, this has been handled by working in the Large N 't Hooft limit [12]. This is useful because the colour charge operators can be decomposed into colour flows, of which some are suppressed by powers of N_c. The suppressed colour flows vanish and the colour structure is greatly simplified to that of colour-anti-colour dipoles with colour lines that do not cross [11]. This is the approach currently implemented in the general purpose event generators, HERWIG [13], Pythia [14] and Sherpa [15, 6].

As will be shown, soft virtual corrections can be decomposed into an Eikonal contribution and a Coulomb contribution. The prior has a structure which matches with real emissions at the cross section level and the latter corresponds to the on shell scattering of a pair of final or initial state partons [5].

Forshaw, Kyrieleis and Seymour developed a framework to systematically account for the non-trivial colour structures of the Coulomb gluons [16, 17, 18]. The algorithm developed is the basis of the work in this thesis and amounts to recursive insertions of real soft emissions each dressed with soft virtual corrections to all orders. They found miscancellations of soft real and virtual Eikonal gluons which gave single non-global logarithms $\alpha_s^m \ln(Q/\rho)^m$ as predicted in [11]. However, cross sections considering 4 or more real emissions were shown to exhibit miscancellations of Coulomb gluons which gave rise to super leading non-global logarithms of the form $\alpha_s^m \ln(Q/\rho)^{m+1}$ [16].

The algorithm rules (see chapter 2) are not Feynman rules but rather a set of effective rules for the leading log calculation of emission of any number of soft gluons.The algorithm was shown in [10] to reproduce the BMS equation [19], a differential evolution equation of leading N parton showers, which itself reproduced the numerical

results of [11]. It has also been shown to be infrared safe. That is, the soft scale, μ can tend to zero without the algorithm diverging.

However, the algorithm has so far not been proven to be collinear safe to all orders. This is the requirement that gluon emissions must be allowed to be collinear with the emitting parton without the observable diverging. Currently, collinear singularities, which arise in the eikonal approximation, are cut from the phase space using Heaviside step functions. These puncture holes of radius λ are centred on singular points and thus cut away every singular region. For the algorithm to be correct, the observables must not depend on the specific value of λ as it is an arbitrary parameter only, introduced to regularise the singularities. If the algorithm gives an observable which diverges as $\lambda \to 0$ then the algorithm must be invalid.

In [10] the colour structures generated using the algorithm are evaluated in the colour flow basis (CFB) [10, 20]. The colour algebra listed above can be represented purely using Kronecker deltas with fundamental indices $i = 1, 2, 3 = R, G, B$ corresponding to the three colour/anti-colour charges quarks and anti-quarks can have. The Kronecker deltas represent quark and anti-quark lines which conserve colour/ anti-colour along the line. In this picture colour structures required for n real emission cross sections are a network of colour and anti-colour lines and vertices through which colour flows and is conserved. The CFB then decomposes amplitudes into weighted sums of distinct colour flows. Using this approach observables can be calculated with full N colour dependence, a significant improvement on the large N limit [20].

In this thesis I calculate the gaps between jets observable up to third order using the FKS algorithm and test for collinear cut-off independence. I describe the FKS algorithm in more detail and define groups of radiation functions ω_{ij}^{k} (see equation 1.7) labelled emission functions, which are generated using the algorithm. These definitions are useful for analytically simplifying the integrals required for higher order observables . I then derive results in the colour flow basis required to evaluate general colour structures. The colour structures for second and third order are given. Using the colour structure results and the emission functions the gaps between jets observable is calculated and simplified as much as possible. I then numerically integrate the expression for a range of λ. The results of which provide strong evidence that

the FKS algorithm is independent of λ at second and third order and the collinear divergences fully cancel.

Chapter 2

The FKS Algorithm

2.1 Feynman Rules to Eikonal Rules

The FKS algorithm is a recursive method of calculating soft (real and virtual) gluon corrections to a hard scattering process. The soft approximation allows for the use of the eikonal rules, a set of simplified Feynman rules and, in turn, the factorisation of the cross section into the original process and the effects of additional soft gluon emissions. The following approximations remain a valid route for calculating a parton shower because of the logarithmic enhancement for soft gluon emissions, that is, for a gluon of momentum k being emitted from a parent parton of momentum p where all elements of k are small compared to the largest component of p.

The algorithm implements soft gluon emissions from quarks, anti-quarks and real gluon legs. Usually the eikonal rules only apply for soft gluon emissions from the hard partons, $q, \bar{q}$ [5]. However, the algorithm applies strong ordering which allows for the assumption that each emission has much lower energy than the previous emission [10]. The relevant Feynman rules are

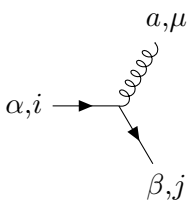

$$= -igt^a_{ji}\gamma^\mu_{\beta\alpha} \tag{2.1}$$

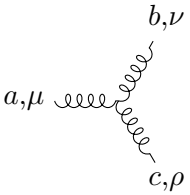

$$= -gf^{abc}\left((p+q)^{\rho}\eta^{\mu\nu} + (q+r)^{\mu}\eta^{\nu\rho} + (r-p)^{\nu}\eta^{\rho\mu}\right) \tag{2.2}$$

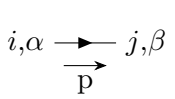

$$= \delta^{ij}\frac{\not{p}_{\alpha\beta} + m}{p^2 - m^2 + i\epsilon} \tag{2.3}$$

where all the usual definitions as seen in the introduction apply. In particular, I have used: lower alphabet greek characters $\alpha, \beta...$ for Dirac indices;middle alphabet greek characters $\mu, \nu...$ for Lorentz indices; lower alphabet characters $a, b...$ for gluon colour indices; and middle alphabet characters $i, j, ...$ for quark line colour indices.

This thesis considers final state radiation dressing the $e^+e^- \to q\bar{q}$ hard scattering process though the following derivation is valid for any hard scattering, $X \to q\bar{q}$. The amplitude for one of the diagrams contributing to $e^+e^- \to q\bar{q}g$ is

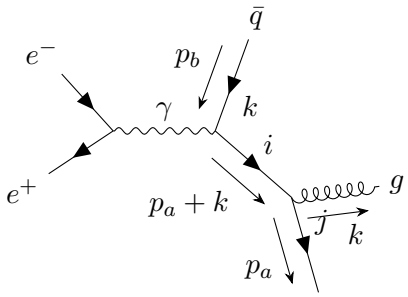

(2.4)

$$\begin{aligned} M \propto & \bar{u}_{\alpha}^{(s_a)}(p_a)\left(-igt_{ij}^{a}\gamma_{\alpha\beta}^{\mu}\right)\epsilon_{\mu}^{*(\lambda)}(k)\left(i\delta_{jk}\frac{\left((p_a+k)_{\rho}\gamma^{\rho}+m\right)_{\beta\gamma}}{(p_a+k)^2 - m^2 + i\epsilon}\right) \\ & \delta_{kl}\gamma_{\gamma\delta}^{\rho}v_{\delta}^{(s_b)}(p_b) \\ & \frac{\eta_{\rho\sigma}}{q^2}\left(u_{\epsilon}^{(s_c)}(p_c)\gamma_{\epsilon\zeta}^{\sigma}\bar{v}_{\zeta}^{(s_d)}(p_d)\right) \end{aligned} \tag{2.5}$$

where I have ignored constants from every term coming from the left of and including the $q\bar{q}\gamma$ vertex. This vertex and all the terms coming from the left of it in the diagram

can be summarized into a single term with the appropriate colour and dirac indices

$$A_{\gamma\delta,kl}(Q) = \sum s_c, s_d \delta_{kl} \gamma^{\rho}_{\gamma\delta} \frac{\eta_{\rho\sigma}}{q^2} \left(u^{(s_c)}_{\epsilon}(p_c)\, \gamma^{\sigma}_{\epsilon\zeta} \bar{v}^{(s_d)}_{\zeta}(p_d) \right) \tag{2.6}$$

where I have ignored a few constants. The amplitude can always be expressed in this form even for more complicated processes. With this definition the amplitude prior to any final state radiation is

$$M_0 \equiv \sum_{s_a, s_b} \bar{u}^{(s_a)}_{\alpha}(p_a)\, A_{\alpha\beta,kl}(Q) v^{(s_b)}_{\beta}(p_b)\,. \tag{2.7}$$

The amplitude with the emission is

$$\begin{aligned} M =& \bar{u}^{(s_a)}_{\alpha}(p_a) \left(-igt^a_{ij} \gamma^{\mu}_{\alpha\beta} \right) \epsilon^{*(\lambda)}_{\mu}(k) \left(i\delta_{jk} \frac{\left((p_a + k)_{\rho} \gamma^{\rho} + m \right)_{\beta\gamma}}{(p_a + k)^2 - m^2 + i\epsilon} \right) \\ & A_{\gamma\delta,kl}(Q) v^{(s_b)}_{\delta}(p_b). \end{aligned} \tag{2.8}$$

In the High Energy limit $p_a^2 = p_b^2 = m_q^2 \approx 0$ and $k^2 = 0$ meaning $(p_a + k)^2 \approx 2p_a \cdot k$. Also, in the soft gluon limit $k \ll p_a$ meaning $p_a + k \approx p_a$. Together, these allow for

$$\frac{\left((p_a + k)_{\rho} \gamma^{\rho} + m \right)_{\beta\gamma}}{(p_a + k)^2 - m^2 + i\epsilon} \approx \frac{\left((p_a)_{\rho} \gamma^{\rho} + m \right)_{\beta\gamma}}{2p.k + i\epsilon} \tag{2.9}$$

which, combined with the spinor relation

$$\left(\not{p}_a + m \right)_{\beta\gamma} = \sum_{s'_a, s_a} u^{(s'_a)}_{\beta}(p_a) \bar{u}^{(s_a)}_{\gamma}(p_a) \tag{2.10}$$

gives

$$\begin{aligned} M =& \sum_{s'_a, s''_a,} \bar{u}^{(s_a)}_{\alpha}(p_a) \left(-igt^a_{ij} \gamma^{\mu}_{\alpha\beta} \right) \epsilon^{*(\lambda)}_{\mu}(k) \left(i\delta_{jk} \frac{u^{(s'_a)}_{\beta}(p_a) \bar{u}^{(s''_a)}_{\gamma}(p_a)}{2p.k + i\epsilon} \right) \\ & A_{\gamma\delta,kl}(Q) v^{(s_b)}_{\delta}(p_b) \\ =& \frac{\left(-igt^a_{ij} \right) \epsilon^{*(\lambda)}_{\mu}(k)}{2p.k + i\epsilon} i \left(\bar{u}^{(s_a)}_{\alpha}(p_a) \gamma^{\mu}_{\alpha\beta} u^{(s'_a)}_{\beta}(p_a) \right) \bar{u}^{(s''_a)}_{\gamma}(p_a) A_{\gamma\delta,jl}(Q) v^{(s_b)}_{\delta}(p_b) \\ =& \frac{\left(-igt^a_{ij} \right) \epsilon^{*(\lambda)}_{\mu}(k)}{2p.k + i\epsilon} i \left(\bar{u}^{(s_a)}_{\alpha}(p_a) \gamma^{\mu}_{\alpha\beta} u^{(s'_a)}_{\beta}(p_a) \right) M_0 \end{aligned} \tag{2.11}$$

where I have used equation 2.7 for M_0. Thus, the effects of a soft gluon emission and the original amplitude can be factorised. Similar derivations can be done for amplitudes where a soft gluon is emitted from incoming and outgoing quarks, anti-quarks and real gluons and the original amplitude is always recovered. The physical interpretation of this result is that low energy emissions (long wavelength) cannot resolve the large energy hard scattering process (short wavelength). This is the fundamental result exploited by the FKS algorithm to recursively build the parton shower.

The terms in the middle set of brackets can be simplified by considering the Dirac equation as follows

$$\begin{aligned}(\not{p}_a - m)u(p_a) =& 0 \\ \not{p}_a u(p_a) =& mu(p_a) \\ \bar{u}(p_a)\not{p}_a u(p_a) =& m\bar{u}(p_a)u(p_a) \\ =& 2m^2\end{aligned} \tag{2.12}$$

also

$$2m^2 = 2p_\mu p^\mu \tag{2.13}$$

meaning

$$\bar{u}(p_a)\gamma^\mu u(p_a) = 2p_a^\mu \tag{2.14}$$

and

$$\left(\bar{u}_\alpha^{(s_a)}(p_a)\gamma^\mu_{\alpha\beta}u_\beta^{(s'_a)}(p_a)\right) = 2p^\mu \delta_{s_a,s'_a} \tag{2.15}$$

which gives the amplitude to be

$$\begin{aligned}M =& \frac{\left(-igt^a_{ij}\right)\epsilon^{*(\lambda)}_\mu(k)}{2p.k + i\epsilon} i2p^\mu M_0 \\ =& \frac{i}{2p.k + i\epsilon} t^a_{ij}\left(-ig2p^\mu\right)\epsilon^{*(\lambda)}_\mu(k) M_0\end{aligned} \tag{2.16}$$

TABLE 2.1: The Eikonal Rules

Direction and Flavour	Propagator	Vertex	Eikonal Feynman Rule
Outgoing Quark	$\frac{i}{2p.k+i\epsilon}$	$t^a_{ij}\,(-i2gp^\mu)\,\epsilon^{*(\lambda)}_\mu(k)$	$\frac{t^a_{ij}gp^\mu\epsilon^{*(\lambda)}_\mu(k)}{p.k+i\epsilon}$
Incoming Quark	$\frac{i}{2p.k-i\epsilon}$	$-t^a_{ji}\,(-i2gp^\mu)\,\epsilon^{*(\lambda)}_\mu(k)$	$\frac{-t^a_{ij}gp^\mu\epsilon^{*(\lambda)}_\mu(k)}{p.k-i\epsilon}$
Outgoing Anti-Quark	$\frac{i}{2p.k+i\epsilon}$	$-t^a_{ji}\,(-i2gp^\mu)\,\epsilon^{*(\lambda)}_\mu(k)$	$\frac{-t^a_{ij}gp^\mu\epsilon^{*(\lambda)}_\mu(k)}{p.k+i\epsilon}$
Incoming Anti-Quark	$\frac{i}{2p.k-i\epsilon}$	$t^a_{ij}\,(-i2gp^\mu)\,\epsilon^{*(\lambda)}_\mu(k)$	$\frac{t^a_{ij}gp^\mu\epsilon^{*(\lambda)}_\mu(k)}{p.k-i\epsilon}$
Outgoing Gluon	$\frac{i}{2p.k+i\epsilon}$	$-if^a_{bc}\,(-i2gp^\mu)\,\epsilon^{*(\lambda)}_\mu(k)$	$\frac{-i\,t^a_{ij}gp^\mu\epsilon^{*(\lambda)}_\mu(k)}{p.k+i\epsilon}$
Incoming Gluon	$\frac{i}{2p.k-i\epsilon}$	$if^a_{cb}\,(-i2gp^\mu)\,\epsilon^{*(\lambda)}_\mu(k)$	$\frac{i\,t^a_{ij}gp^\mu\epsilon^{*(\lambda)}_\mu(k)}{p.k-i\epsilon}$

leading to the eikonal propagator and vertex factor rules for the emission from a quark flavoured external parton

$$\frac{i}{2p.k+i\epsilon}\,,\; t^a_{ij}\,(-ig2p^\mu)\,\epsilon^{*(\lambda)}_\mu(k). \tag{2.17}$$

Similar derivations can be done for the other flavours of radiating partons. For example, the eikonal rules derivation for radiation from an outgoing anti-quark can be found in [5, 21]. The eikonal rules are listed in table 2.1. Because e^+e^- are colour neutral I am considering final state radiation only. Therefore, only the outgoing eikonal rules are relevant here. The FKS algorithm can be applied to initial state radiation for which the incoming eikonal rules would be relevant.

2.2 Real Corrections

The amplitude prior to radiation is recovered no mater how many soft gluons are considered meaning the eikonal rules above can be applied any number of times to produce a shower of n soft gluons. The difference is that with each emission the number of real legs from which radiation can occur grows by one. To build a gauge invariant cross section one must calculate the modulus squared of the sum of all diagrams which contribute to an observable. Therefore, each application of the recursion relation systematically inserts an emission from every real leg of the shower.

Using the results from table 2.1 the operator to insert a soft emission from parton i is

$$\boldsymbol{T}_i^a \frac{i}{2p_i \cdot k + i\epsilon} (-i2gp_i^\mu)\ \epsilon_\mu^{*(\lambda)}(k) = g\,\boldsymbol{T}_i^a \frac{p_i^\mu}{p_i \cdot k + i\epsilon} \epsilon_\mu^{*(\lambda)} \tag{2.18}$$

where the notation $\boldsymbol{T}_i^a$ refers to the colour charge operator for a parton i emitting a gluon a. The colour charge operators for different flavour partons are listed in the brackets of the eikonal vertex factors (see table 2.1). Equation 2.18 is applied to every real leg of the shower such that, in bra-ket notation,

$$\begin{aligned} |M_n\rangle &= \sum_j g\mathbf{T}_j^{a_n} \frac{p_j^\nu}{p_j \cdot k} \epsilon_\nu^{*(\lambda_n)} |M_{n-1}\rangle \\ &\equiv J_n^{\dagger a_n} |M_{n-1}\rangle \end{aligned} \tag{2.19}$$

where I have used the definition of the soft gluon current, J, as used in [10]. Similarly, the conjugate amplitude is evolved using

$$\begin{aligned} \langle M_n| &= \langle M_{n-1}| \sum_i g\mathbf{T}_i^{\dagger a_n} \frac{p_i^\nu}{p_i \cdot k} \epsilon_\nu^{(\lambda_n)} \\ &\equiv \langle M_{n-1}|\, J_n^{a_n} \end{aligned} \tag{2.20}$$

where the hermitian conjugate of the polarization vector and colour charge have been used, the momentum terms remain unchanged.

The polarization vectors for gluons at the same level of evolution from the amplitude and conjugate amplitude share polarization indices and momentum dependence. Diagrammatically the gluons lines link in the amplitude squared diagrams. Therefore, at the amplitude squared level the completeness relation for physical gluon polarization states

$$\sum_T \epsilon_\nu^{(T)}(p_n)\epsilon_\mu^{*(T)}(p_n) = -\eta_{\mu,\nu}, \tag{2.21}$$

where T denotes transverse polarisation states, can be applied and the the 4-momenta from each eikonal vertex are contracted. The sum over physical polarisations (T) can be replaced by the metric up to corrections beyond the leading log approximation [5].

The four momentum of the emitted soft gluon must then be integrated over the Lorentz invariant phase space. Only the region where the gluon is soft compared to

the hard process will give logarithmic enhancements meaning we can safely cut the upper limit of the integral at hard scale, Q. Furthermore, the gluon is constrained to be on-shell as it is an external gluon, giving

$$\begin{aligned}\int dLIPS_k &\approx \int^Q \frac{d^4k}{(2\pi)^4}\delta(k^2) \\ &= \int^Q \frac{d^3\underline{k}}{(2\pi)^3 2E_k} \\ &= \frac{\alpha_s}{g^2\pi}\int^Q \frac{dE_k}{E_k}\int \frac{d\Omega_k}{4\pi}E_k^2\end{aligned} \tag{2.22}$$

where the dirac delta functions imposing conservation of momentum have already been applied in the derivation of the eikonal rules i.e. $q(p+k) \to q(p)+g(k)$. Beyond this point in the derivation we used the approximation of $p+k \approx p$ which allows for the integration over the additional gluon momentum to be factorised from the rest of the phase space. Corrections to this approximation are known as recoil effects.

At the cross section level, the above two results lead to the formation of the radiation function, ω_{ij}^k. This is defined as

$$\omega_{ij}^k \equiv \frac{E_k^2 p_i \cdot p_j}{p_i \cdot p_k p_j \cdot p_k} \tag{2.23}$$

in [1, 10, 5] and corresponds to an insertion of an emission joining leg i of the amplitude and leg j of the conjugate amplitude or vice versa. The emitting legs are all external and are therefore on-shell which has the consequences

$$p_i \cdot p_j = p_i^2 = m_i^2 \approx 0, i = j \tag{2.24}$$

and

$$\omega_{ii}^k = \frac{p_i^2}{(p_i \cdot p_k)^2} \approx 0 \tag{2.25}$$

for real radiation functions (radiation functions for virtual corrections are discussed below). Furthermore, we can express the momenta as

$$p_\mu \equiv (p_0, p_1, p_2, p_3) = (E, \underline{p}) = E(1, \underline{n}) = En_\mu \tag{2.26}$$

where $\underline{n}$ is the 3-dimensional unit vector pointing in the direction of $\underline{p}$. This gives

$$\begin{aligned}\omega_{ij}^{k} &\equiv \frac{E_k^2 p_i \cdot p_j}{p_i \cdot p_k p_j \cdot p_k} \\ &= \frac{E_k^2 E_i E_j n_i \cdot n_j}{E_k^2 E_i E_j n_i \cdot n_k n_j \cdot n_k} \\ &= \frac{n_i \cdot n_j}{n_i \cdot n_k n_j \cdot n_k}\end{aligned} \tag{2.27}$$

meaning the radiation function is a function of the directions of the partons involved only. This identifies the two collinear poles

$$n_{i,j} \cdot n_k \xrightarrow{\underline{n}_{i,j} \cdot \underline{n}_k = 1} n_{i,j} \cdot n_k = 1 - 1 = 0. \tag{2.28}$$

Note that, due to the fundamental and adjoint representations of $SU(3)_c$ being hermitian, the colour algebra terms for these links obey

$$\begin{aligned}\sum_a \boldsymbol{T}_i^{\dagger a} \boldsymbol{T}_j^a &= \boldsymbol{T}_i \cdot \boldsymbol{T}_j \\ &= \sum_a \boldsymbol{T}_j^{\dagger a} \boldsymbol{T}_i^a \\ &= \sum_a \boldsymbol{T}_j^a \boldsymbol{T}_i^a \\ &= \sum_a \boldsymbol{T}_j^{\dagger a} \boldsymbol{T}_i^{\dagger a}\end{aligned} \tag{2.29}$$

where the dot product definition is used in [5, 16, 10].

The amplitude squared $\langle M_n | M_n \rangle$ is then a sum of diagrams where all possible pairs of emitting partons ij from the previous amplitude and conjugate amplitude are linked by the real gluon line. Explicitly, the cross section for the insertion of the n^{th}

soft gluon is

$$\begin{aligned}
\sigma_n &= \int dLIPS_n \langle M_n | M_n \rangle \\
&= \int dLIPS_{n-1} \sum_{i,j,a_n,\lambda_n} \int^Q \frac{d^4 p_n}{(2\pi)^4} \delta(p_n^2) \langle M_{n-1} | J_n^{\dagger a_n} \cdot J_n^{a_n} | M_{n-1} \rangle \\
&= \int dLIPS_{n-1} \frac{\alpha_s}{g^2 \pi} \int^Q \frac{E_n^2 dE_n}{E_n} \int \frac{d\Omega}{4\pi} \\
&\sum_{i,j,a_n,\lambda_n} \langle M_{n-1} | g \mathbf{T}_i^{\dagger a_n} \frac{p_i^\nu}{p_i \cdot p_n} \epsilon_\nu^{(\lambda_n)} g \mathbf{T}_j^{a_n} \frac{p_j^\mu}{p_j \cdot p_n} \epsilon_\mu^{*(\lambda_n)} | M_{n-1} \rangle \\
&= \int dLIPS_{n-1} \frac{\alpha_s}{g^2 \pi} \int^Q \frac{E_n^2 dE_n}{E_n} \int \frac{d\Omega}{4\pi} \\
&\sum_{i,j} \langle M_{n-1} | g^2 \mathbf{T}_i \cdot \mathbf{T}_j \frac{p_i^\nu}{p_i \cdot p_n} (-\eta_{\mu\nu}) \frac{p_j^\mu}{p_j \cdot p_n} | M_{n-1} \rangle \\
&= - \int dLIPS_{n-1} \frac{\alpha_s}{\pi} \int^Q \frac{dE_n}{E_n} \int \frac{d\Omega_n}{4\pi} \sum_{i,j} \langle M_{n-1} | \mathbf{T}_i \cdot \mathbf{T}_j \frac{E_n^2 p_i \cdot p_j}{p_i \cdot p_n p_j \cdot p_n} | M_{n-1} \rangle \\
&= - \int dLIPS_{n-1} \frac{\alpha_s}{\pi} \int^Q \frac{dE_n}{E_n} \int \frac{d\Omega_n}{4\pi} \sum_{i,j} \langle M_{n-1} | \mathbf{T}_i \cdot \mathbf{T}_j | M_{n-1} \rangle \omega_{ij}^n
\end{aligned} \tag{2.30}$$

where I have used equations 2.22, 2.23 and 2.29.

In general the colour charge operators from each level of the evolution cannot join in this way, it is only those from the last emission that can. The non-abelian quality of $SU(3)_c$ means the colour charge operators cannot commute past the previous and subsequent emission terms. The string of colour charge operators is collectively known as the colour structure. Chapter 3 is dedicated to analysing the colour structure for up to 3 emissions and discusses how the FKS algorithm does so up to any order using the colour flow basis. The Lorentz space, labeled by indices $\mu, \nu...$, is distinct from the colour space meaning for every real emission the momentum terms can commute past the colour algebra to form a sum of radiation functions, ω_{ij}^k, weighted by colour factors, C_{ij}, which are not, in general, equivalent to $\boldsymbol{T}_i \cdot \boldsymbol{T}_j$. This allows for the complete factorisation of the previous differential cross section element and the probability of a real soft gluon emission

$$d\sigma_n = d\sigma_{n-1} \left(- \frac{\alpha_s}{\pi} \frac{dE_n}{E_n} \frac{d\Omega_n}{4\pi} \sum_{i,j} C_{ij} \omega_{ij}^n \right). \tag{2.31}$$

which is referred to as soft factorisation [1].

2.3 Virtual Corrections

The effect of virtual gluons in the shower is to exchange colour between real legs i.e. to alter the colour structure. The eikonal rules from table 2.1 are still valid for these diagrams except the internal gluon propagator inserts an extra $\frac{-i}{k^2+i\epsilon}$ factor and absorbs the polarization vectors from each eikonal vertex. The momentum of the internal gluon line, k, circulates around the loop created by the internal line meaning it is not an observable and must therefore be integrated over all possible momenta. This means propagators from the emitting real legs having opposite signs to accommodate the flow of momentum. Therefore, the amplitude with an inserted virtual correction between every pair of partons i, j is

$$\begin{aligned}
|M_n^{(1)}\rangle =& \sum_{i<j} \int \frac{d^4k}{(2\pi)^4} g\mathbf{T}_i^{a_n} \frac{p_i^\mu}{-p_i\cdot k + i\epsilon} \frac{-i\eta_{\mu\nu}}{k^2+i\epsilon} g\mathbf{T}_j^{a_n} \frac{p_j^\nu}{p_j\cdot k + i\epsilon} |M_n^{(1)}\rangle \\
=& \sum_{i<j} -i \int \frac{d^4k}{(2\pi)^4} \mathbf{T}_i\cdot\mathbf{T}_j g^2 p_i\cdot p_j \frac{1}{(-p_i\cdot k+i\epsilon)(k^2+i\epsilon)(p_j\cdot k+i\epsilon)} |M_n^{(1)}\rangle \\
\equiv& I_n^{a_n} |M_n^{(0)}\rangle
\end{aligned} \tag{2.32}$$

where the sum is over partons $i < j$ instead of i, j to prevent double counting and I have used the notation $I_n^{a_n}$ from [5]. Note also that self energy graphs, where $i = j$, do not contribute to the cross sections in the Feynman gauge for reasons outlined in equation 2.25.

The integral can be simplified by performing a contour integral around the singularities which have been perturbed from the real axis into the complex plane of k_0 using the $i\epsilon$ prescription. The relevant integral is then

$$\begin{aligned}
&\int \frac{dk_o}{2\pi} \frac{1}{((p_i-k)^2+i\epsilon)((k)^2+i\epsilon)((p_j+k)^2+i\epsilon)} \\
&= \int \frac{dk_o}{2\pi} \frac{1}{(-p_i\cdot k+i\epsilon)(k^2+i\epsilon)(p_j\cdot k+i\epsilon)} \\
&= \int \frac{dk_o}{2\pi} \frac{1}{(-k_0 p_{i0} + \underline{p}_i\cdot\underline{k}+i\epsilon)(k_0+|\underline{k}|+i\epsilon)(k_0-|\underline{k}|-i\epsilon)(k_0 p_{j0} - \underline{p}_j\cdot\underline{k}+i\epsilon)}
\end{aligned} \tag{2.33}$$

which has poles at

$$k_0 = (\frac{\underline{p}_i \cdot \underline{k}}{p_{i0}} + i\epsilon), (-E_k - i\epsilon), (E_k + i\epsilon), (\frac{\underline{p}_j \cdot \underline{k}}{p_{j0}} - i\epsilon) \tag{2.34}$$

where I have used $E_k = |\underline{k}|$. Closing the contour to include the positive half of the imaginary axis encompasses the first and third poles in the list and using Cauchy's residue theorem gives

$$\begin{aligned}
&\int \frac{dk_o}{2\pi} \frac{1}{((p_i - k)^2 + i\epsilon)((k)^2 + i\epsilon)((p_j + k)^2 + i\epsilon)} \\
&= -i2\pi \frac{1}{2\pi(k^2 + i\epsilon)((\frac{\underline{p}_i \cdot \underline{k}}{p_{i0}} p_{j0} - \underline{p}_j \cdot \underline{k} + i\epsilon)} \\
&- i2\pi \frac{1}{2\pi(-E_k p_{i0} + \underline{p}_i \cdot \underline{k} + i\epsilon)(k_0 + E_k + i\epsilon)(E_k p_{j0} - \underline{p}_j \cdot \underline{k} + i\epsilon)} \\
&= \frac{-i}{(k^2 + i\epsilon)((\frac{\underline{p}_i \cdot \underline{k}}{p_{i0}} p_{j0} - \underline{p}_j \cdot \underline{k} + i\epsilon)} + \frac{-i}{2E_k(-p_i \cdot k)(p_j \cdot k)} \\
&= \frac{-i}{(k^2 + i\epsilon)((\frac{\underline{p}_i \cdot \underline{k}}{p_{i0}} p_{j0} - \underline{p}_j \cdot \underline{k} + i\epsilon)} + \frac{i}{2E_k(p_i \cdot k)(p_j \cdot k)}
\end{aligned} \tag{2.35}$$

The residue with $k_0 = E_k$ corresponds to the gluon propagator going on-shell and gives the following real valued term in the full virtual correction function

$$\begin{aligned}
R_n = Re[I_n] &= \sum_{i<j} -i \int \frac{d^3k}{(2\pi)^3} \mathbf{T}_i \cdot \mathbf{T}_j g^2 p_i \cdot p_j \frac{i}{2E_k(p_i \cdot k)(p_j \cdot k)} \\
&= \sum_{i<j} \int \frac{d^3k}{2E_k(2\pi)^3} \mathbf{T}_i \cdot \mathbf{T}_j g^2 p_i \cdot p_j \frac{1}{(p_i \cdot k)(p_j \cdot k)} \\
&= \sum_{i<j} \frac{\alpha}{\pi} \int \frac{dE_k}{E_k} \int \frac{d\Omega_k}{4\pi} \mathbf{T}_i \cdot \mathbf{T}_j p_i \cdot p_j \frac{1}{(p_i \cdot k)(p_j \cdot k)} \\
&= -\frac{\alpha}{\pi} \sum_{i<j} \int \frac{dE_k}{E_k} \int \frac{d\Omega_k}{4\pi} (-\mathbf{T}_i \cdot \mathbf{T}_j) \omega_{ij}^k
\end{aligned} \tag{2.36}$$

which is known as the radiative or Eikonal virtual gluon contribution as it exhibits the same structure as equation 2.30. Note, however the relative difference of $-\frac{1}{2}$. The sign difference originates from the conservation of momentum flowing into the second eikonal vertex (i.e. $-p_i \cdot p_k$ instead of $p_i \cdot p_k$). Here I have chosen the gluon momentum to flow into parton i but the above argument is valid for choosing parton j, the important point is that the two propagators should have opposite signs. The factor of a half is due to the pair ij being a distinct contribution from ji in the real

radiation equation but is considered the same event for the virtual radiation and so is not included to prevent double counting.

The remaining term from equation 2.35 can be shown to evaluate to a complex term of the form

$$A_n \equiv Im[I_n] = -\frac{\alpha_s}{\pi}\sum_{i<j}\int\frac{dE_k}{E_k}\int\frac{d\Omega_k}{4\pi}(-\mathbf{T}_i\cdot\mathbf{T}_j)(-i\pi)\tilde{\delta}_{ij} \tag{2.37}$$

where $\tilde{\delta}_{ij} = 1$ if partons i, j are both incoming or outgoing and 0 otherwise [5]. This thesis concerns the e^+e^- hard process which can only give rise to final state radiation as the incoming particles are colour neutral. I can therefore set $\tilde{\delta}_{ij} = 1$. The imaginary term is referred to as the Coulomb or absorptive gluon (hence A_n).

The amplitude for the insertion of a virtual gluon between every real leg in the shower amplitude can now be written

$$I_n\left|M_n\right\rangle = R_n\left|M_n\right\rangle + A_n\left|M_n\right\rangle \tag{2.38}$$

and the corresponding operation for the conjugate amplitude is

$$\begin{aligned}\left\langle M_n\right| I_n^\dagger &= \left\langle M_n\right| R_n^\dagger + \left\langle M_n\right| A_n^\dagger \\ &= \left\langle M_n\right| R_n - \left\langle M_n\right| A_n\end{aligned} \tag{2.39}$$

where I have used equation 2.29 and the fact only A_n is imaginary. This leads to cancellations of the absorptive term between certain pairs of squared amplitude terms. For example, the cross section for the bare scattering dressed with one virtual gluon is the sum of the amplitude and conjugate sides being dressed

$$\begin{aligned}\sigma_0^{(1)} &= \int dLIPS_0\left\langle M_0\right| I_0\left|M_0\right\rangle + \left\langle M_0\right| I_0^\dagger\left|M_0\right\rangle \\ &= \int dLIPS_0\left\langle M_0\right| R_0\left|M_0\right\rangle + \left\langle M_0\right| A_0\left|M_0\right\rangle + \left\langle M_0\right| R_0^\dagger\left|M_0\right\rangle + \left\langle M_0\right| A_0^\dagger\left|M_0\right\rangle \\ &= \int dLIPS_0\left\langle M_0\right| R_0\left|M_0\right\rangle + \left\langle M_0\right| A_0\left|M_0\right\rangle + \left\langle M_0\right| R_0^\dagger\left|M_0\right\rangle - \left\langle M_0\right| A_0\left|M_0\right\rangle \\ &= \int dLIPS_0 2\left\langle M_0\right| R_0\left|M_0\right\rangle .\end{aligned} \tag{2.40}$$

Chapter 3 will show how cancellations of this type occur for the first three orders. At fourth order there is miscancellation which leads to the super leading logs [16, 17].

The virtual correction is then applied to all orders using the Sudakov factor. This describes the probability of the shower not radiating between certain energy scales [1]. In the algorithm these two scales are the scales of the previous and subsequent real emission. It is the sum of products of I_n

$$\begin{aligned}\boldsymbol{V}_{E_{n+1},E_n} &= 1 + \int_{E_{n+1}}^{E_n} \frac{dE_k}{E_k} f(\Omega_k) + \int_{E_{n+1}}^{E_n} \frac{dE_k}{E_k} f(\Omega_k) \int_{E_{n+1}}^{E_k} \frac{dE_{k+1}}{E_{k+1}} f(\Omega_{k+1}) + \cdots \\ &= \exp\left[\int_{E_{n+1}}^{E_n} \frac{dE_k}{E_k} f(\Omega_k)\right] \\ &= \exp\left[I_n\right]\end{aligned} \tag{2.41}$$

where $f(\Omega_k)$ refers to everything in I_n except the energy integral.

2.4 The Algorithm Rules

The algorithm applies the operators J_i and V_{E_{i+1},E_i} to recursively build up the number of gluons considered in the cross sections for parton shower observables. This systematically inserts real gluon emissions from every real leg in the shower and dresses the subsequent shower with virtual corrections between each real parton up to any order. The modulus squared amplitude is written in trace form to make calculations of the colour factors easier (see chapter 3) and the real emissions are integrated over Lorentz invariant phase space weighted with a measurement function specific to an observable.

A general observable calculated up to p^{th} order is

$$\Sigma^{(p)}(\mu) = \int \sum_{n=0}^{p} d\sigma_n^{(p)} u_n\left(k_1, k_2, \cdots, k_n\right) \tag{2.42}$$

where $d\sigma_n^{(p)}$ is the differential cross section for n real emissions and $p-n$ virtual corrections. For GBJ, which is our focus, the measurement function, $u_n\left(k_1, k_2, \cdots, k_n\right)$, acts to veto certain regions of the phase space and as such consists of Heaviside theta functions which are unity in the accepted region and zero otherwise. The real emission

phase space is weighted by these, as in equation 2.42, but the virtual phase space is not. Written out in full, the algorithm evolves the differential cross section as follows

$$d\sigma_n = Tr\left(\boldsymbol{V}_{E_{n+1},E_n}\boldsymbol{D}_n^{\mu}\cdots\boldsymbol{V}_{E_2,E_1}D_1^{\nu}\boldsymbol{V}_{E_1,Q}\boldsymbol{H}(Q)\boldsymbol{V}^{\dagger}_{E_1,Q}\boldsymbol{D}^{\dagger}_{1\nu}\boldsymbol{V}^{\dagger}_{E_2,E_1}\cdots\boldsymbol{D}^{\dagger}_{n\mu}\boldsymbol{V}^{\dagger}_{E_{n+1},E_n}\right) d\Pi_1 d\Pi_2\cdots d\Pi_n \tag{2.43}$$

where

$$\mathbf{D}_i^{\mu} = \sum_j \mathbf{T}_j E_i \frac{p_j^{\mu}}{p_j\cdot q_i}\Theta_{cut} \tag{2.44}$$

inserts real emissions. This is effectively the soft gluon current, $\boldsymbol{J}_i$ except it includes an energy factor and an uncontracted momentum term destined to form radiation functions ω_{ij}^k when contracted with the momentum part of the corresponding $\boldsymbol{D}^{\dagger}$.The Θ_{cut} term is product of Heaviside step functions which puncture holes in the phase space of radius λ around unit vectors collinear to the emitting partons. In this case there is only one collinear singularity but Θ_{cut} is used generally as

$$\Theta_{cut} = \prod_{i,k}\Theta\left(n_k\cdot n_i-\lambda\right). \tag{2.45}$$

where i and k label the parton and gluon. The aim of this thesis is to calculate the effects of allowing $\lambda\to 0$. The Sudakov factor is

$$\boldsymbol{V}_{E_{i+1},E_i} = P\exp\left[-\frac{\alpha_s}{\pi}\int_{E_{i+1}}^{E_i}\frac{dE_k}{E_k}\left(\sum_{i<j}-\boldsymbol{T}_i\cdot\boldsymbol{T}_j\right)\int\frac{d\Omega_k}{4\pi}\omega_{ij}^k\Theta_{cut}+A_i\right] \tag{2.46}$$

where I have kept the absorptive (Coulomb) term unspecified as it will be shown to cancel for the cases I am considering. The Sudakov factors following D_i dress the shower after i emissions with virtual corrections up to all orders. Expansion of the exponential up to the m^{th} order and selecting the m^{th} order terms corresponds to dressing the real legs of the shower amplitude with m virtual gluons in all combinations possible.

The phase space element is that of a real emission meaning equation 2.30 can always be used. This gives

$$d\Pi_i \equiv -\frac{\alpha_s}{\pi}\frac{dE_i}{E_i}\frac{d\Omega_i}{4\pi}. \tag{2.47}$$

Strong energy ordering has been implemented by assuming the most energetic gluon can be considered first followed by lower energy gluons and so on. This is imposed by setting the upper integral limit equal to the energy of the previous emission. The reasoning for using this assumption is detailed in [10]. This algorithm has been derived in a basis-independent notation of $SU(3)_c$ and only universal properties of the group have been used, specifically that elements of the group must be hermitian.

2.5 The Gaps between Jets observable

The gaps between jets observable vetoes emissions into the angular region between the two cones centred on the back to back quarks as illustrated in figure 2.1. This means u_n can be factorised into n Heaviside functions which make the appropriate cuts on the phase space for each real gluon emission

$$u_n\left(q_1,\ldots,q_n\right) = \prod_{i=1}^{n} u_1\left(q_i\right) \tag{2.48}$$

$$u_1(k) = \Theta_{out}(k) + \Theta_{in}\Theta(\rho > E_k) \tag{2.49}$$

where $\Theta_{out}(k)$ is unity if k is in the out of gap region and $\Theta_{in}\Theta(\rho > E_k)$ is unity if k is in the gap region and has energy below the experimental cut off ρ [10]. For reasons outlined in the introduction we can effectively set $\rho = \mu$.

The measurement function therefore affect the real emission phase space as follows

$$\begin{aligned}\int d\Pi_1 \cdots \int d\Pi_n f\left(\Omega_1,\Omega_2,\cdots,\Omega_n\right) u_n\left(n_1\cdots n_n\right) = \left(-\frac{\alpha_s}{\pi}\right)^n \int_\mu^Q \frac{dE_1}{E_1}\cdots\int_\mu^{E_{n-1}} \frac{dE_n}{E_n} \\ \int_{Out}\frac{d\Omega_1}{4\pi}\cdots\int_{Out}\frac{d\Omega_n}{4\pi} \\ f\left(\Omega_1,\Omega_2,\cdots,\Omega_n\right)\Theta_{cut}\end{aligned} \tag{2.50}$$

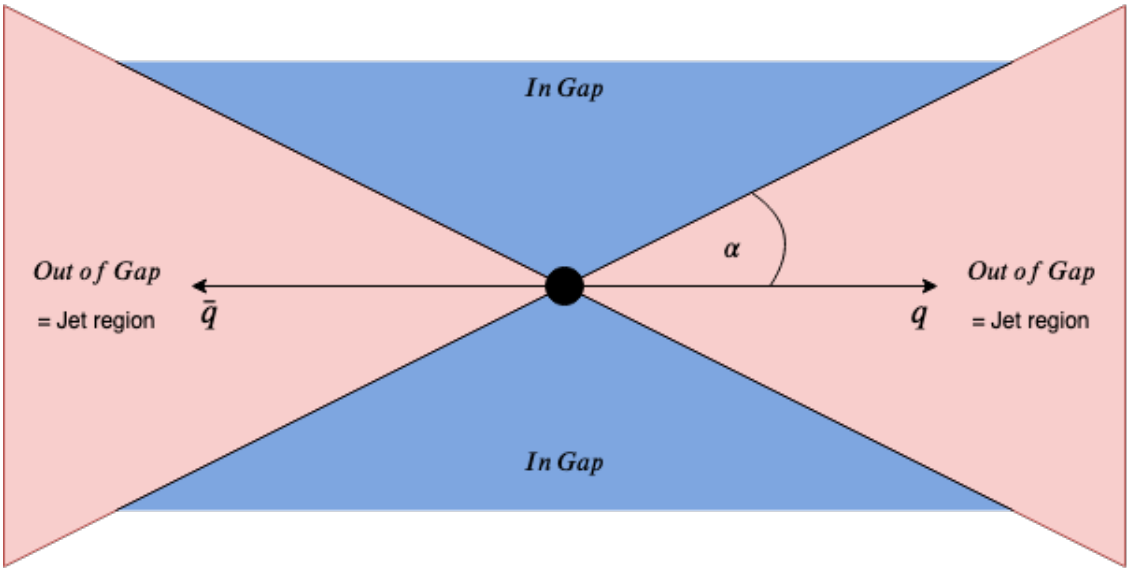

FIGURE 2.1: Diagram to illustrate the regions of the phase space. *In Gap* is the vetoed region in-between the back to back jets. *Out of Gap* is the region occupied by the jets. α is the opening angle of the jets from the back to back quark-anti-quark pair.

where *Out* refers region out of the gap between back to back jets of opening angle α, i.e. the out region is the jet region

$$\begin{aligned}\int_{\text{Out}} \frac{d\Omega_i}{4\pi} f(\Omega_i)\,\Theta_{cut} &= \int_0^{\alpha} \frac{d\theta_i \sin(\theta_i)}{2} \int_0^{2\pi} \frac{d\phi_i}{2\pi} f(\Omega_i)\,\Theta_{cut} \\ &+ \int_{\pi-\alpha}^{\pi} \frac{d\theta_i \sin(\theta_i)}{2} \int_0^{2\pi} \frac{d\phi_i}{2\pi} f(\Omega_i)\,\Theta_{cut} \\ &= \int_c^1 \frac{dx_i}{2} \int_0^{2\pi} \frac{d\phi_i}{2\pi} f(\Omega_i)\,\Theta_{cut} \\ &+ \int_{-1}^{-c} \frac{dx_i}{2} \int_0^{2\pi} \frac{d\phi_i}{2\pi} f(\Omega_i)\,\Theta_{cut} \\ &\equiv \ddot{f}(\Omega_i)\end{aligned} \tag{2.51}$$

where $x_i \equiv \cos(\theta_i)$ and $c \equiv \cos(\alpha)$.

Similarly, a function integrated over the region in the gap is

$$\begin{aligned}\int_{\text{in}} \frac{d\Omega_i}{4\pi} f(\Omega_i)\,\Theta_{cut} &= \int_{\alpha}^{\pi-\alpha} \frac{d\theta_i \sin(\theta_i)}{2} \int_0^{2\pi} \frac{d\phi_i}{2\pi} f(\Omega_i)\,\Theta_{cut} \\ &= \int_c^{-c} \frac{dx_i}{2} \int_0^{2\pi} \frac{d\phi_i}{2\pi} f(\Omega_i)\,\Theta_{cut} \\ &\equiv \dot{f}(\Omega_i)\,.\end{aligned} \tag{2.52}$$

Finally a function integrated over the entire region is defined

$$\begin{aligned}\int_{all} \frac{d\Omega_i}{4\pi} f(\Omega_i)\,\Theta_{cut} &= \int_0^{\pi} \frac{d\theta_i \sin(\theta_i)}{2} \int_0^{2\pi} \frac{d\phi_i}{2\pi} f(\Omega_i)\,\Theta_{cut} \\ &= \int_{-1}^{1} \frac{dx_i}{2} \int_0^{2\pi} \frac{d\phi_i}{2\pi} f(\Omega_i)\,\Theta_{cut} \\ &\equiv \bar{f}(\Omega_i)\end{aligned} \tag{2.53}$$

meaning

$$\begin{aligned}\bar{f}(\Omega_i) &= \ddot{f}(\Omega_i) + \dot{f}(\Omega_i) \\ all &= out + in.\end{aligned} \tag{2.54}$$

The emissions are ordered in energy such that the most energetic gluon is considered first, hence we have the energy integrals

$$\int_{\mu}^{E_0 \equiv Q} \frac{dE_1}{E_1} \int_{\mu}^{E_1} \frac{dE_2}{E_2} \cdots \int_{\mu}^{E_{n-1}} \frac{dE_n}{E_n} \tag{2.55}$$

for a shower involving n emissions. This integral can be simplified using

$$t_i \equiv \ln\left(\frac{E_i}{\mu}\right) \tag{2.56}$$

leading to

$$\int_0^{t_0} dt_1 \int_0^{t_1} dt_2 \cdots \int_0^{t_{n-1}} dt_n. \tag{2.57}$$

This notation can be extended to simplify the energy integrals included in the Sudakov factors. The energy of each virtual gluon is integrated between the energy of the previous real emission energy scale, E_i, and that of the next, E_{i+1}. The integral simplifies to

$$\begin{aligned}\int_{E_{i+1}}^{E_i} \frac{dE_k}{E_k} &= \ln\left(\frac{E_i}{E_{i+1}}\right) \\ &= \ln\left(\frac{E_i}{\mu}\right) - \ln\left(\frac{E_{i+1}}{\mu}\right) \\ &= t_i - t_{i+1} \\ &\equiv \acute{t_i}\end{aligned} \tag{2.58}$$

where $\acute{t_i}$ has been defined. This definition holds for the final, n^{th}, Sudakov if we define the lower energy limit, E_{n+1} to be the soft scale, μ. It follows that

$$\begin{aligned}\acute{t_n} &= \ln\left(\frac{E_n}{\mu}\right) - \ln\left(\frac{\mu}{\mu}\right) \\ &= \ln\left(\frac{E_n}{\mu}\right)\end{aligned} \tag{2.59}$$

which matches with

$$\int_\mu^{E_n} \frac{dE_k}{E_k}. \tag{2.60}$$

In this form the energy ordered expansion of the Sudakov subsequent to the n^{th} real emission up to p^{th} order has a structure similar to the real emission energy ordering

$$\int_0^{\acute{t_n}} dx_1 \int_0^{x_1} dx_2 \cdots \int_0^{x_{p-1}} dx_p = \frac{\acute{t_n}^p}{p!} \tag{2.61}$$

which holds because the rest of the exponent has no energy dependence.

It is also helpful to define an expression to include the colour factors linked with the corresponding ω functions for Eikonal virtual gluons

$$F_m^{(k)} \equiv \left(\sum_{i<j} -T_i \cdot T_j \omega_{ij}^k \right) \tag{2.62}$$

where the upper (k) index labels the gluon number which, for virtuals, starts at one above the real emission number. For example, the first virtual gluon considered in a shower with 2 real emissions will have a label of $k = 3$. However, this doesn't mean it was emitted below the two real gluons in the energy scale. The lower index of F dictates at what point in the shower evolution the virtual gluon was exchanged. $F_0^{(k)}$ acts to exchange a virtual gluon between the quark anti-quark legs prior to emissions. $F_1^{(k)}$ is the sum of all the ways a gluon can be exchanged between the real shower legs after 1 real emission, $F_2^{(k)}$ is for after 2 real emissions and so on. It is true then for any $F_m^{(k)}$ function that $m < k$. Virtual Eikonal gluons are integrated over the entire phase space as follows

$$\bar{F}_m^{(k)} \equiv \left(\sum_{i<j} -T_i \cdot T_j \int_{all} \frac{d\Omega_k}{4\pi} \omega_{ij}^k \Theta_{cut} \right) \tag{2.63}$$

which, combined with equations 2.58 and 2.46, allows for the Sudakov factor with no Coulomb gluon terms to be written as

$$V_{E_{m+1},E_m} = \exp\left[-\frac{\alpha_s}{\pi} t_m' \bar{F}_m \right]. \tag{2.64}$$

It is useful to consider the trace of a cross section with no virtual corrections

$$\epsilon_m^{(1,\cdots,m)} \equiv \mathrm{Tr}\left(D_m^\mu \cdots D_1^\nu H(Q) D_{1\nu}^\dagger \cdots D_{m\mu}^\dagger \right) \tag{2.65}$$

where the upper index lists the gluons considered in the trace and the lower index is the number of real emissions. Due to the cyclicity of the trace

$$\epsilon_m^{(1,\cdots,m)} \equiv \mathrm{Tr}\left(D_{m\mu}^\dagger D_m^\mu \cdots D_1^\nu H(Q) D_{1\nu}^\dagger \cdots D_{m-1\mu}^\dagger \right). \tag{2.66}$$

The $D_m^\dagger D_m$ combination can be simplified as follows

$$\begin{aligned} D_{m\mu}^\dagger D_m^\mu &= \sum_{i,j}^{m-1} \mathbf{T}_i^{\dagger(m)} \frac{n_{i\mu}}{n_i \cdot n_m} \mathbf{T}_j^{(m)} \frac{n_j^\mu}{n_j \cdot n_m} \\ &= \sum_{i\neq j}^{m-1} \mathbf{T}_i^{\dagger(m)} \mathbf{T}_j^{(m)} \omega_{ij}^m \\ &= 2 \sum_{i<j}^{m-1} T_i \cdot T_j \omega_{ij}^m \\ &= -2F_{m-1}^{(m)} \end{aligned} \tag{2.67}$$

where I have used the result that the gluons are on shell and therefore $\omega_{ii} = 0$. I have also used

$$T_i \cdot T_j \equiv T_i^{\dagger(m)} T_j^{(m)} \tag{2.68}$$

where the (m) in both charge operators indicated they describe the addition of the same gluon and the colour lines therefore link when taking the trace.

Finally, the virtual colour-momentum structures, F, can be extracted from the trace by defining

$$\begin{aligned} f_m^{(k)} &\equiv \frac{\mathrm{Tr}\left(F_m^k D_m^\mu \cdots D_{m\mu}^\dagger\right)}{\mathrm{Tr}\left(D_m^\mu \cdots D_{m\mu}^\dagger\right)} \\ &= \frac{\mathrm{Tr}\left(F_m^k D_m^\mu \cdots D_{m\mu}^\dagger\right)}{\epsilon_m^{(1,\cdots,m)}} \end{aligned} \tag{2.69}$$

which allows for

$$\mathrm{Tr}\left(F_m^{(k)} D_m^\mu \cdots D_{m\mu}^\dagger\right) = \epsilon_m^{(1,\cdots,m)} f_m^{(k)} \tag{2.70}$$

and, in turn

$$\begin{aligned} \epsilon_{m+1}^{(1,\cdots,m,m+1)} &= \mathrm{Tr}\left(D_{m+1}^\nu D_m^\mu \cdots D_{m\mu}^\dagger D_{m+1\nu}^\dagger\right) \\ &= \mathrm{Tr}\left(D_{m+1\nu}^\dagger D_{m+1}^\nu D_m^\mu \cdots D_{m\mu}^\dagger\right) \\ &= \mathrm{Tr}\left(-2F_m^{(m+1)} D_m^\mu \cdots D_{m\mu}^\dagger\right) \\ &= -2\epsilon_m^{(1,\cdots,m)} f_m^{(m+1)} \end{aligned} \tag{2.71}$$

which is true for any value of m.

Using the emission functions (EFs) ϵ, f or F to calculate cross sections can lead to some explicit cancellations of entire groups of $T_i \cdot T_j \omega_{ij}^k$ terms. Likewise, using the

hatted emission functions (HEFs), marked by $-, \cdot$ or $\cdot\cdot$, helps to recognise cancellations of the EFs in specific regions of the phase space (see equation 2.54). However, cross sections written in this way are strings of multiple HEFs and care must be taken when manipulating them to find cancellations and when converting the result back to standard integration notation. This section discusses what manipulations are consistent with equation 2.43.

Firstly, in general, the integration coupled with each ϵ, f or F, marked by $-, \cdot$ or $\cdot\cdot$ must include the entire cross section structure in the integrands as in 2.43. For example, if $k \neq l$

$$\ddot{X}^{(l)}\dot{Y}^{(k)} \equiv \int_{Out} \frac{d\Omega_l}{4\pi} \int_{In} \frac{d\Omega_k}{4\pi} X^{(l)} Y^{(k)} \tag{2.72}$$

rather than

$$\left[\int_{Out} \frac{d\Omega_1}{4\pi} X^{(l)}\right] \left[\int_{In} \frac{d\Omega_k}{4\pi} Y^{(k)}\right] \tag{2.73}$$

where X and Y are generic emission functions. In other words HEFs are not necessarily factorisable, in contrast to ϵ and f. This is because $Y^{(k)}$ ($X^{(l)}$) could, (and often does), have Ω_l (Ω_k) dependence.

This is the normal situation because EFs depend on the momenta of the emitting partons. No gluons are emitted from virtual gluons meaning no other functions will be dependent on their solid angle and the integration associated with these functions must be completed first. The real EFs will be dependant on the solid angles of the earlier emissions so integrals associated with the real emission must be ordered from last to first. Hence the integration for a multiplicity p observable must be ordered

$$\int \frac{d\Omega_1}{4\pi} \int \frac{d\Omega_2}{4\pi} \cdots \int \frac{d\Omega_p}{4\pi}, \tag{2.74}$$

as in 2.43. This region of each integral is tracked by the type of hat and the upper index of each HEF.

The order of integration can be altered in some cases. For example, the order of the virtual integrals is arbitrary for the reason mentioned above. This corresponds to being able to switch the upper indices of $\bar{f}_m^{(k)}$. A general cross section with virtuals at stages a and b where $a, b \in 1, ..., m$ has the structure

$$
\begin{aligned}
\ddot{X}^{(1,\cdots,m)}\bar{f}_a^{(k)}\bar{f}_b^{(l)} \equiv & \int_{Out}\frac{d\Omega_1}{4\pi}\cdots\int_{Out}\frac{d\Omega_m}{4\pi}\int_{All}\frac{d\Omega_k}{4\pi}\int_{All}\frac{d\Omega_l}{4\pi} \\
& X^{(1,\cdots,m)}(\Omega_1\cdots\Omega_m)f_a^{(k)}(\Omega_1\cdots\Omega_m,\Omega_k)f_b^{(l)}(\Omega_1\cdots\Omega_m,\Omega_l) \\
& = \left[\int_{Out}\frac{d\Omega_1}{4\pi}\cdots\int_{Out}\frac{d\Omega_m}{4\pi}X^{(1,\cdots,m)}(\Omega_1,\cdots,\Omega_m)\right. \\
& \left.\left[\int_{All}\frac{d\Omega_k}{4\pi}f_a^{(k)}(\Omega_1\cdots\Omega_a,\Omega_k)\right]\left[\int_{All}\frac{d\Omega_l}{4\pi}f_b^{(l)}(\Omega_1\cdots\Omega_b,\Omega_l)\right]\right] \\
& = \left[\int_{Out}\frac{d\Omega_1}{4\pi}\cdots\int_{Out}\frac{d\Omega_m}{4\pi}X^{(1,\cdots,m)}(\Omega_1,\cdots,\Omega_m)\right. \\
& \left.\left[\int_{All}\frac{d\Omega_l}{4\pi}f_b^{(l)}(\Omega_1\cdots\Omega_b,\Omega_l)\right]\left[\int_{All}\frac{d\Omega_k}{4\pi}f_a^{(k)}(\Omega_1\cdots\Omega_a,\Omega_k)\right]\right] \\
& = \ddot{X}^{(1,\cdots,m)}\bar{f}_b^{(l)}\bar{f}_a^{(k)}
\end{aligned}
\tag{2.75}
$$

where in the second to last line the dummy indices of l and k have just been switched. This means the virtual f functions can commute past each other. By similar reasoning

$$
\begin{aligned}
\ddot{X}^{(1,\cdots,m)}\bar{f}_m^{(k)}\ddot{f}_m^{(l)} \equiv & \int_{Out}\frac{d\Omega_1}{4\pi}\cdots\int_{Out}\frac{d\Omega_m}{4\pi}\int_{All}\frac{d\Omega_k}{4\pi}\int_{Out}\frac{d\Omega_l}{4\pi} \\
& X^{(1,\cdots,m)}(\Omega_1\cdots\Omega_m)f_m^{(k)}(\Omega_1\cdots\Omega_m,\Omega_k)f_m^{(l)}(\Omega_1\cdots\Omega_m,\Omega_l) \\
& = \int_{Out}\frac{d\Omega_1}{4\pi}\cdots\int_{Out}\frac{d\Omega_m}{4\pi}X^{(1,\cdots,m)}(\Omega_1,\cdots,\Omega_m) \\
& \left[\int_{All}\frac{d\Omega_k}{4\pi}f_m^{(k)}(\Omega_1\cdots\Omega_m,\Omega_k)\right]\left[\int_{Out}\frac{d\Omega_l}{4\pi}f_m^{(l)}(\Omega_1\cdots\Omega_m,\Omega_l)\right] \\
& = \int_{Out}\frac{d\Omega_1}{4\pi}\cdots\int_{Out}\frac{d\Omega_m}{4\pi}X^{(1,\cdots,m)}(\Omega_1,\cdots,\Omega_m) \\
& \left[\int_{Out}\frac{d\Omega_l}{4\pi}f_m^{(l)}(\Omega_1\cdots\Omega_m,\Omega_l)\right]\left[\int_{All}\frac{d\Omega_k}{4\pi}f_m^{(k)}(\Omega_1\cdots\Omega_m,\Omega_k)\right] \\
& = \ddot{X}^{(1,\cdots,m)}\ddot{f}_m^{(l)}\bar{f}_m^{(k)}
\end{aligned}
\tag{2.76}
$$

i.e. the two f_m functions integrated over different regions can commute past each other provided the lower index matches.

Chapter 3

Colour Structure Calculations

3.1 Colour Structure Calculations

The FKS algorithm detailed in the last chapter gives a sum of amplitudes, squared. This is written in trace form and integrated over the appropriate phase space for a given observable. This chapter will describe how the trace is calculated. The Dirac and Lorentz matrices can commute past the colour algebra meaning each pair of $\boldsymbol{D}_n^\mu \cdots \boldsymbol{D}_{\mu n}^\dagger$ terms gives a sum of radiation functions ω_{ij}^n where ij are all the distinct pairs of real legs in the shower at that point. The colour charge operators $\boldsymbol{T}_i$ and $\boldsymbol{T}_j^\dagger$ coupled to the momentum parts remain in place of the full $\boldsymbol{D}$ terms. Similarly, from the radiative virtual gluon contribution $\boldsymbol{R}_n$ we can extract $-\omega_{ij}^k$ and leave $\boldsymbol{T}_i \cdot \boldsymbol{T}_j$. For the purposes of this section I will assume the absorptive terms from the virtuals cancel and do not need to be considered.

For example, a subset of the cross section diagrams at third order are those corresponding to 2 real emissions and 1 virtual correction occurring between the scales of the first and second emission on the amplitude side. The trace giving this sum of diagrams is

$$\mathrm{Tr}[\boldsymbol{D}_2^\mu \boldsymbol{F}_1^{(3)} \boldsymbol{D}_1^\nu \boldsymbol{H} \boldsymbol{D}_{1\nu}^\dagger \boldsymbol{D}_{2\mu}^\dagger] \tag{3.1}$$

where for the time being I have ignored the factor of $\frac{-\alpha_s {t_1}'}{\pi}$ and the integration over E_k, Ω_k from the Sudakov. The Coulomb term would give a trace structure identical to this but would have a factor of $i\pi$ instead of$-\omega_{kl}^3$ inside $\boldsymbol{F}_1^{(3)}$. The hard scattering matrix has also been set to the identity matrix as we are considering a colour singlet

production process. Expanding the terms out gives

$$\sum_{\{ij\},\{k<l\},\{mn\}} \mathrm{Tr}[\boldsymbol{T}_m\boldsymbol{T}_k \cdot \boldsymbol{T}_l\boldsymbol{T}_i\boldsymbol{T}_j^\dagger\boldsymbol{T}_n^\dagger]\,\omega_{ij}^1\omega_{mn}^2(-\omega_{kl}^3) \tag{3.2}$$

where

$$\begin{aligned} \{ij\} &= ab, ba \\ \{mn\} &= ab, ba, a1, 1a, b1, 1b \\ \{k<l\} &= ab, a1, b1. \end{aligned} \tag{3.3}$$

Note, we choose to label the real gluons before the virtual gluons even if the virtual is emitted at a higher energy scale than the real emission [10].

Equations such as the one above are sometimes referred to as an antenna patterns [1] as they describe how the shower can branch outwards and the colour factor weights associated with each branching. The above antenna pattern is just one in the set which contribute to the third order calculation. Others are the patterns where the virtual gluon is inserted in a different position in the trace or patterns where there are a different number of virtuals and reals. In general, they will have a structure similar to that of equation 3.2 with a product of n radiation functions and a colour structure factor consisting of a trace of $2n$ colour charge operators where n is the order of the calculation.

At this point a representation for the $SU(3)_c$ algebra must be chosen to evaluate the value of the colour structure. One contribution to the antenna pattern of equation 3.2 considers the legs

$$i = a,\ j = b,\ k = a,\ l = b,\ m = 1,\ n = a \tag{3.4}$$

where leg a is the quark leg, b is the anti-quark leg and all numbered legs correspond to gluons. Figure 3.1 contains the diagram for the colour structure.

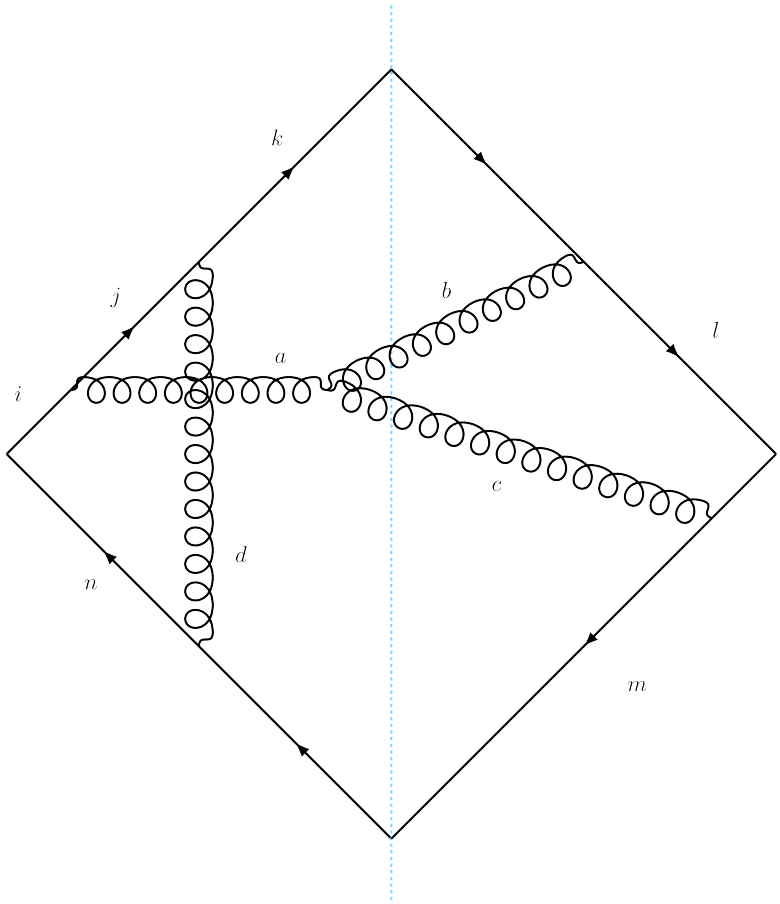

FIGURE 3.1: A cross section level diagram displaying the colour structure for one configuration of 2 real emissions and 1 virtual correction occurring between the scales of the first and second emission.

Using the fundamental and adjoint representations, equation 3.2 evaluates to

$$\mathrm{Tr}[\boldsymbol{T}_1\boldsymbol{T}_a\cdot\boldsymbol{T}_b\boldsymbol{T}_a\boldsymbol{T}_b^\dagger\boldsymbol{T}_a^\dagger]\,\omega_{ab}^1\omega_{a1}^2(-\omega_{ab}^3)=\mathrm{Tr}[if^{abc}(-\boldsymbol{t}_{kj}^d\boldsymbol{t}_{nm}^d)\boldsymbol{t}_{ji}^a\boldsymbol{t}_{ml}^c\boldsymbol{t}_{lk}^b]\omega_{ab}^1\omega_{a1}^2(-\omega_{ab}^3) \tag{3.5}$$

where I have used the results from table 2.1 for the colour charge operators. The correct assignment of the fundamental and adjoint indices (i, j, k, l, m and a, b, c, d respectively) requires drawing the colour structure diagram which is not easily automated. Calculating the trace once the indices are labelled then involves the application of numerous identities. For large multiplicity cross sections, this algebra quickly becomes intractable by hand and difficult to automate.

3.2 Colour Algebra Diagrams

A quicker and more intuitive approach to evaluating the trace is to use diagrams. The diagrammatic rules are derived by expressing the colour algebra terms in the fundamental basis using

$$if^{abc} = 2\mathrm{Tr}[[\boldsymbol{t}^a, \boldsymbol{t}^b]\boldsymbol{t}^c] \tag{3.6}$$

and then expressing the Gell-Mann matrices as combinations of Kronecker deltas such that the properties of the group hold. Specifically, we can express the octet representation of $SU(3)_c$ as a nonet with the over-counted singlet state removed [4]. The Kronecker deltas can then be expressed diagrammatically using quark or anti-quark lines which carry a colour and anti-colour index respectively. The diagram identities required for this work are:

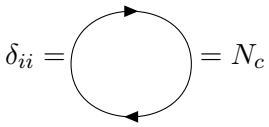

(3.7a)

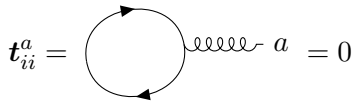

(3.7b)

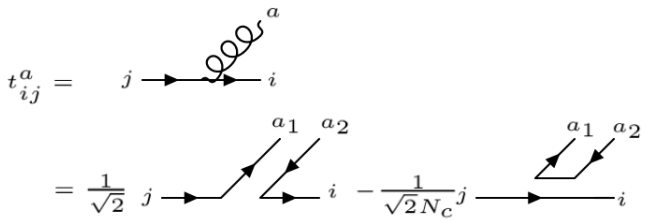

(3.7c)

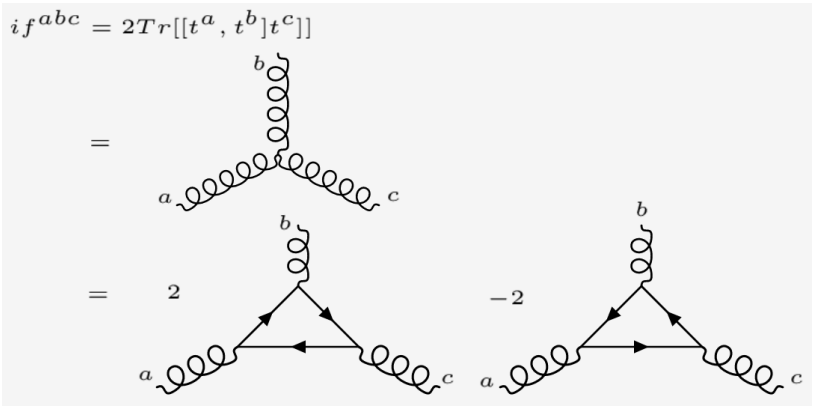

(3.7d)

These diagrams can then be used to arrive at the Fierz identity and the alternative representation of the structure constants, if^{abc}:

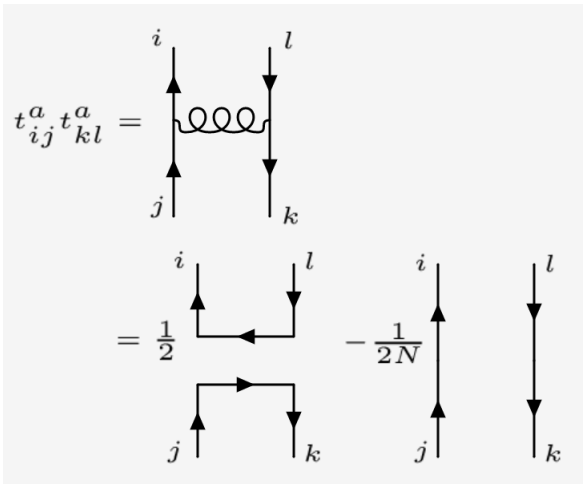

(3.8a)

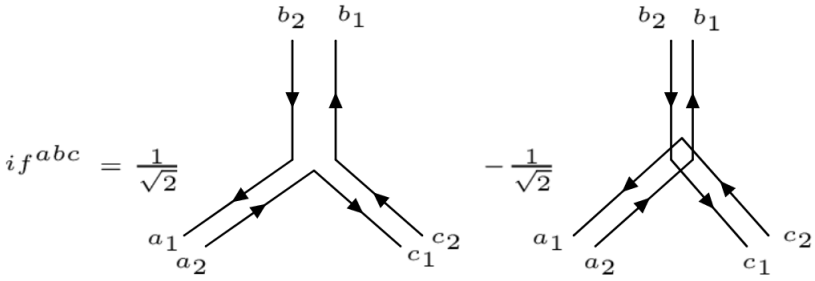

(3.8b)

Colour operator products can then be evaluated. $\boldsymbol{T}_a \cdot \boldsymbol{T}_b$ between the hard scattering process and the first emission and $\boldsymbol{T}_a \cdot \boldsymbol{T}_b$ and $\boldsymbol{T}_a \cdot \boldsymbol{T}_1$ between the first and

second emission are given by:

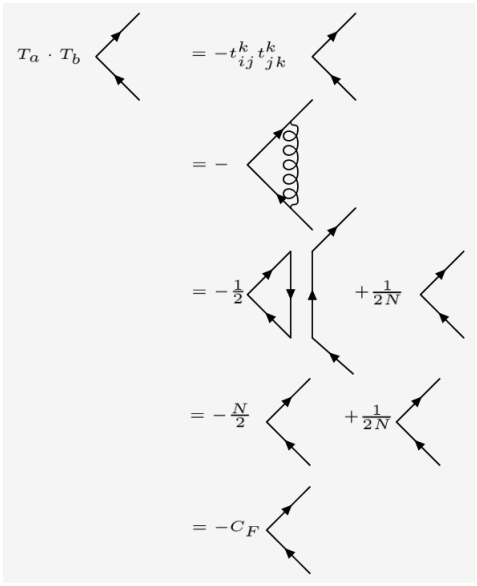

(3.9a)

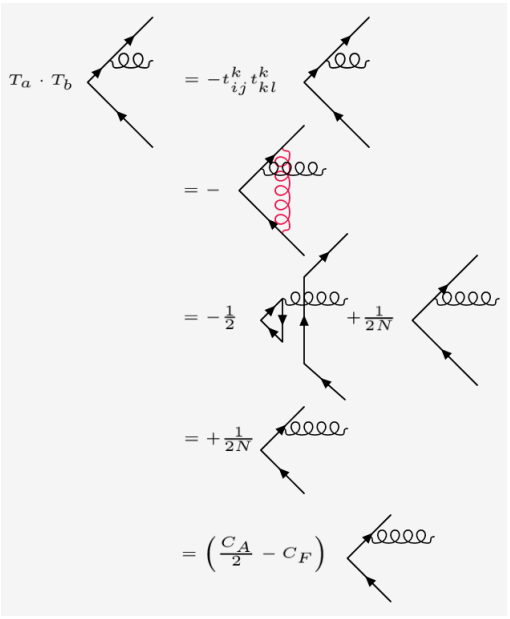

(3.9b)

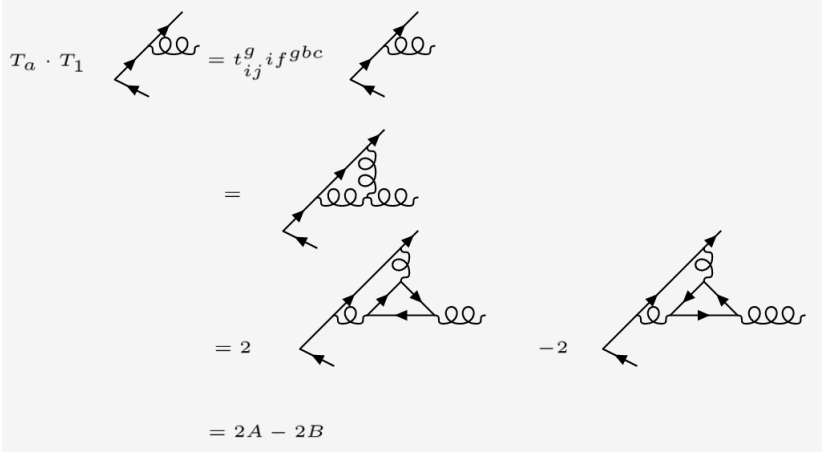

(3.9c)

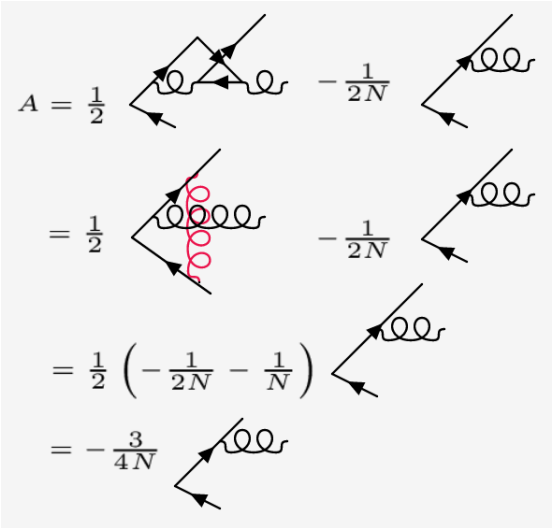

(3.9d)

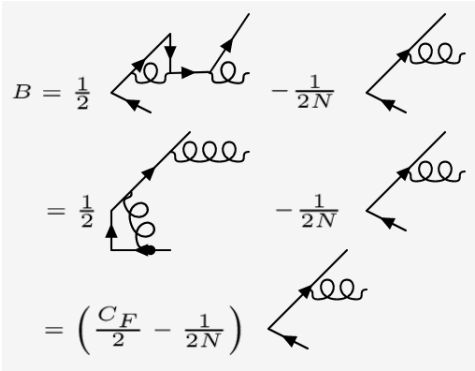

(3.9e)

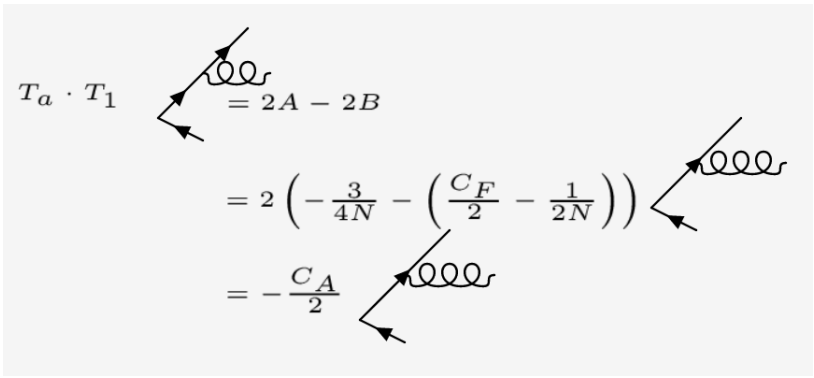

(3.9f)

where the factors of -1 in the first two diagrams are due to the colour charge operator at the anti-quark leg. The red gluon is coloured differently only for clarity to emphasise there is no vertex at the crossing of the gluons. After the colour charge operators have been applied, the diagrams make no distinction between the quark and anti-quark lines leaving the hard scattering vertex, it is a single colour line. Each of the operators act to reproduce the original colour structure diagram with a constant prefactor. They are therefore group invariants and proportional to the identity matrix. The same can be shown for $\boldsymbol{T}_b \cdot \boldsymbol{T}_1$. The operators $\boldsymbol{T}_a \cdot \boldsymbol{T}_b$ above

the scale of the first emission and $\boldsymbol{T}_a \cdot \boldsymbol{T}_b$, $\boldsymbol{T}_a \cdot \boldsymbol{T}_1$ and $\boldsymbol{T}_b \cdot \boldsymbol{T}_1$ above the scale of the second emission are abelian which means $\boldsymbol{F}_0$ and $\boldsymbol{F}_1$ are also abelian and can be moved around and extracted from the trace. These qualities are used extensively in the next chapter.

Using these results the colour structure of figure 3.1 can be quickly evaluated:

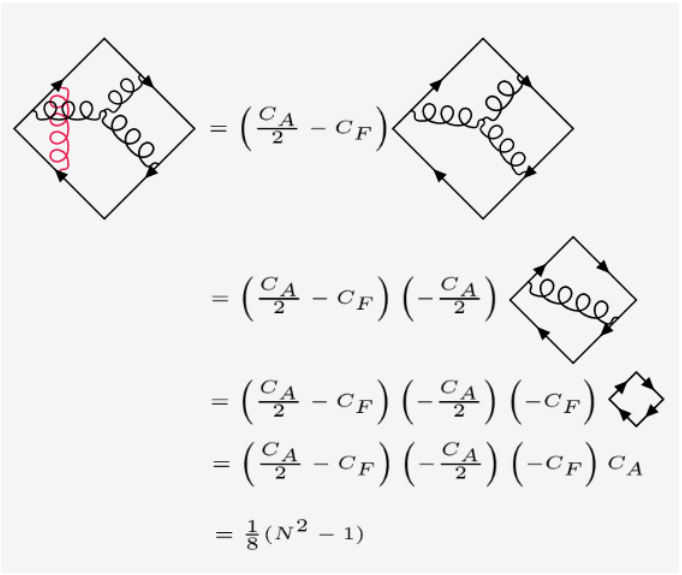

(3.10)

where I have included the effects of the factor of -1 coming from $\boldsymbol{T}_b$. In this fashion, these diagrams allow for the evaluation of arbitrarily complex colour structures. Once a diagram has been evaluated, it can be used to calculate higher order diagrams and this can be repeated indefinitely. However, equation 3.5 is just one of many colour structures to be calculated at third order. Therefore, up to the orders required for parton shower resummations, calculating the colour structures in this way remains impractical.

One approach used in the past is to calculate in the large N 't Hooft limit [12]. This sets the number of colours to be $N \gg 1$ which suppresses the colour singlet term in the Fierz identity. Calculations using this limit are said to be Leading N [4].

3.3 The Colour Flow Basis

The Colour Flow Basis (CFB) decomposes amplitudes into weighted sums of all possible routes external anti-colour lines can flow to external colour lines in the colour structure. This choice of representation for the $SU(3)_c$ algebra provides a method of

calculating colour structures up to any order whilst maintaining full colour dependence or expanding in terms of N [20].

The approach is related to the diagrammatic approach and uses the results described in the previous section. Consider equation 3.8a, each diagrammatic term represents a different route the colour or anti-colour lines can take. In the CFB each of these terms is a basis tensor. In this way, amplitudes are described as a sum of the basis tensors weighted by a product of the colour algebra factors (T_R, N_c , N_g etc.) and any other factors that apply to the entire colour structure.

The quark (anti-quark) carries colour (anti-colour) meaning it is represented by a colour (anti-colour) leg. Gluons carry both colour and anti-colour meaning each real gluon emission adds a colour leg and anti-colour leg. An amplitude with n real emissions therefore has $n+1$ colour and $n+1$ anti-colour legs. Each basis tensor is defined as a product of Kronecker deltas which link the fundamental indices of external colour legs with external anti-colour legs in a distinct way. In other words each basis tensor for an amplitude with n pairs of legs is a permutation of the list $1, ..., n$ and as such is one of $n!$ tensors. The tensors are defined as

$$\begin{aligned} |\sigma\rangle \equiv & |\sigma(1)\cdots\sigma(m)\rangle \\ = & \delta^{\alpha_1}_{\bar{\alpha}_{\sigma(1)}} \cdots \delta^{\alpha_m}_{\bar{\alpha}_{\sigma(1)}} \end{aligned} \tag{3.11}$$

where the upper indices are the fundamental colour indices of the i^{th} colour leg and the lower indices are the fundamental anti-colour indices. Amplitudes are then given by

$$|M\rangle = \sum_{\sigma} M_\sigma |\sigma\rangle \tag{3.12}$$

where the sum is over the set of permutations. Conjugate basis tensors are given by

$$\begin{aligned} \langle\sigma| \equiv & \langle\sigma(1)\cdots\sigma(m)| \\ = & \delta^{\bar{\alpha}_{\sigma(1)}}_{\alpha_1} \cdots \delta^{\bar{\alpha}_{\sigma(m)}}_{\alpha_m}. \end{aligned} \tag{3.13}$$

where the position i in the bra indicates which colour line the anti-colour line $\bar{c}_{\sigma(i)}$ flows to. The inner product is then

$$\langle\tau|\sigma\rangle = \delta^{\bar{\alpha}_{\tau(1)}}_{\alpha_1} \cdots \delta^{\bar{\alpha}_{\tau(m)}}_{\alpha_m} \delta^{\alpha_1}_{\bar{\alpha}_{\sigma(1)}} \cdots \delta^{\alpha_m}_{\bar{\alpha}_{\sigma(m)}}. \tag{3.14}$$

If two permutations differ by one transposition such that $\tau(i) = \sigma(j)$, $\tau(j) = \sigma(i)$, the inner product is

$$\begin{aligned}\langle\tau|\sigma\rangle =& \delta^{\bar{\alpha}_{\tau(1)}}_{\alpha_1} \delta^{\alpha_1}_{\bar{\alpha}_{\sigma(1)}} \cdots \delta^{\bar{\alpha}_{\tau(i)}}_{\alpha_i} \delta^{\alpha_i}_{\bar{\alpha}_{\sigma(i)}} \delta^{\bar{\alpha}_{\tau(j)}}_{\alpha_j} \delta^{\alpha_j}_{\bar{\alpha}_{\sigma(j)}} \cdots \delta^{\bar{\alpha}_{\tau(m)}}_{\alpha_m} \delta^{\alpha_m}_{\bar{\alpha}_{\sigma(m)}} \\ =& \delta^{\bar{\alpha}_{\tau(1)}}_{\bar{\alpha}_{\tau(1)}} \cdots \delta^{\bar{\alpha}_{\tau(i)}}_{\bar{\alpha}_{\tau(i)}} \cdots \delta^{\bar{\alpha}_{\tau(m)}}_{\bar{\alpha}_{\tau(m)}} \\ =& N^{n-1}\end{aligned} \tag{3.15}$$

where every pair of Kronecker deltas contracts to give a factor of N except for the four involved with the transposition which all contract to give just one factor of N. This happens for each transposition meaning, in general

$$\mathcal{S}_{\tau\sigma} \equiv \langle\tau|\sigma\rangle = N^{n-\#\mathrm{trans}(\sigma,\tau)} \tag{3.16}$$

where $\#\mathrm{trans}(\sigma,\tau)$ is the number of transpositions between the two permutations and the scalar product matrix, $\mathcal{S}_{\tau\sigma}$, has been defined. The CFB tensors are therefore non-orthogonal.

This means basis independent operators such as the colour charge operators cannot be represented solely using the basis. Projecting operators onto the basis states to calculate the matrix elements leads to contradictions, in general we have

$$\begin{aligned}\boldsymbol{R} &= \sum_{\sigma,\tau} \langle\sigma|\boldsymbol{R}|\tau\rangle |\sigma\rangle\langle\tau| \\ &= \sum_{\sigma,\tau,\alpha,\beta} \langle\sigma|\langle\alpha|\boldsymbol{R}|\beta\rangle|\alpha\rangle\langle\beta||\tau\rangle|\sigma\rangle\langle\tau| \\ &= \sum_{\sigma,\tau,\alpha,\beta} \langle\alpha|\boldsymbol{R}|\beta\rangle\langle\sigma||\alpha\rangle\langle\beta||\tau\rangle|\sigma\rangle\langle\tau| \\ &= \sum_{\sigma,\tau,\alpha,\beta} \langle\alpha|\boldsymbol{R}|\beta\rangle N^{2n-\#\mathrm{trans}(\sigma,\alpha)-\#\mathrm{trans}(\beta,\tau)} |\sigma\rangle\langle\tau| \\ &\neq \sum_{\sigma,\tau} \langle\sigma|\boldsymbol{R}|\tau\rangle|\sigma\rangle\langle\tau|.\end{aligned} \tag{3.17}$$

To remedy this, a dual basis is introduced which has the defining properties

$$\begin{aligned} \mathbf{I} =& |\alpha]\langle\alpha| = |\alpha\rangle[\beta| \\ \delta_{\alpha\beta} =& \langle\alpha|\,\beta] = [\beta\,|\alpha\rangle \end{aligned} \tag{3.18}$$

which allows for operators to be defined as

$$\begin{aligned} \boldsymbol{R} =& \sum_{\sigma,\tau} [\sigma|\boldsymbol{R}|\tau]\,|\sigma\rangle\langle\tau| \\ =& \sum_{\sigma,\tau} \mathcal{R}_{\sigma\tau}\,|\sigma\rangle\langle\tau| \end{aligned} \tag{3.19}$$

where $\mathcal{R}_{\sigma\tau}$ are the dual basis matrix elements not the matrix elements of the basis independent operator $\boldsymbol{R}$. This definition is now self-consistent because

$$\begin{aligned} \boldsymbol{R} =& \sum_{\sigma,\tau} [\sigma|\boldsymbol{R}|\tau]\,|\sigma\rangle\langle\tau| \\ =& \sum_{\sigma,\tau,\alpha,\beta} [\sigma|[\alpha|\boldsymbol{R}|\beta]\,|\alpha\rangle\langle\beta|\,\tau]\,|\sigma\rangle\langle\tau| \\ =& \sum_{\sigma,\tau,\alpha,\beta} \mathcal{R}_{\alpha\beta}[\sigma\,|\alpha\rangle\langle\beta|\,\tau]\,|\sigma\rangle\langle\tau| \\ =& \sum_{\sigma,\tau,\alpha,\beta} \mathcal{R}_{\alpha\beta}\delta_{\sigma\alpha}\delta_{\beta\tau}\,|\sigma\rangle\langle\tau| \\ =& \sum_{\sigma,\tau} \mathcal{R}_{\sigma\tau}\,|\sigma\rangle\langle\tau|\,. \end{aligned} \tag{3.20}$$

To calculate colour structures we need to evaluate objects such as

$$\mathrm{Tr}[\boldsymbol{A}] = \mathrm{Tr}[\boldsymbol{L}\boldsymbol{H}\boldsymbol{R}] \tag{3.21}$$

where $\boldsymbol{H} = |M_0\rangle\langle M_0|$ is the hard scattering matrix, $\boldsymbol{L}$ is a product of colour charge operators evolving the amplitude colour structure and $\boldsymbol{R}$ evolves the conjugate amplitude colour structure. The trace is the sum of diagonal terms of the operator sandwiched between orthogonal basis tensors:

$$\mathrm{Tr}[\boldsymbol{A}] = \sum_{\rho} [\rho|\boldsymbol{A}\,|\rho\rangle \tag{3.22}$$

inserting the identity matrix and using equation 3.19 gives

$$\begin{aligned}\mathrm{Tr}[\boldsymbol{A}] =& \sum_{\rho,\sigma} [\rho|\boldsymbol{A}|\sigma] \langle\sigma|\rho\rangle \\ =& \sum_{\rho,\sigma} \mathcal{A}_{\rho\sigma}\mathcal{S}_{\sigma\rho} \\ =& \mathrm{Tr}[\mathcal{A}\mathcal{S}]\end{aligned} \tag{3.23}$$

where the scalar product matrix $\mathcal{S}_{\sigma\rho}$ corrects for the non-orthogonality of the basis. The matrix elements $\mathcal{A}_{\rho\sigma}$ contain the evolution of the colour structure.

These matrix elements are calculated by inserting the identity to recursively strip and evaluate the outermost colour charge operators until the Hard Scattering matrix is reached. For example:

$$\begin{aligned}[\rho|\boldsymbol{A}|\sigma] &= [\rho|\boldsymbol{L}\boldsymbol{H}\boldsymbol{R}|\sigma] \\ &= \sum_{\alpha\beta} [\rho|\boldsymbol{L}\,|\alpha\rangle\,[\alpha|\boldsymbol{H}|\beta]\,\langle\beta|\,\boldsymbol{R}|\sigma] \\ &= \sum_{\alpha\beta} [\alpha|\boldsymbol{H}|\beta][\rho\,|\alpha'\rangle\,\boldsymbol{C}_L^{\alpha}C_R^{\beta}\,\langle\beta'|\,\sigma] \\ &= \sum_{\alpha\beta} [\alpha|\boldsymbol{H}|\beta]\delta_{\rho\alpha'}\delta_{\beta'\sigma}\boldsymbol{C}_L^{\alpha}\boldsymbol{C}_R^{\beta} \\ &= \sum_{\alpha\beta} [\alpha|\,|H\rangle\,\langle H|\,|\beta]\delta_{\rho\alpha'}\delta_{\beta'\sigma}\boldsymbol{C}_L^{\alpha}\boldsymbol{C}_R^{\beta}\end{aligned} \tag{3.24}$$

where $\boldsymbol{C}_L^{\alpha}$ and $\boldsymbol{C}_R^{\beta}$ are a set of constants generated after evolving the colour flow α and β using operators $\boldsymbol{L}$ and $\boldsymbol{R}$. The Kronecker deltas force the permutations ρ and σ to match α' and β' i.e. those arrived at by evolving α with $\boldsymbol{L}$ and β with $\boldsymbol{R}$. From this point I will refer to terms such as $[\rho|\boldsymbol{L}\,|\alpha\rangle \equiv \delta_{\rho\alpha'}\boldsymbol{C}_L^{\alpha}$ as matrix elements of the operator $\boldsymbol{L}$.

3.4 Real Corrections

By relabelling the indices in equations 3.7c, 3.8b the specific form of the colour charge operators in the Colour Flow basis can be determined. For an emission from a quark

line:

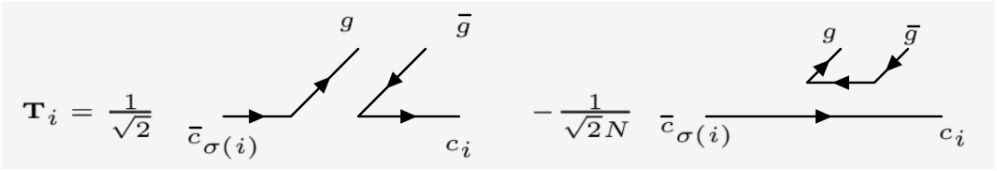

(3.25)

where $\bar{c}_{\sigma(i)}$ is the anti-colour line from which the quark's colour flowed prior to the emission. The index c_i is the colour line of the quark. The first term acts to insert a colour line g and an anti-colour line $\bar{g}$ such that colour flows from $\bar{c}_{\sigma(i)}$ to g and from $\bar{g}$ to c_i. In CFB tensor notation this is equivalent to appending an element at the end of the permutation list and the switching it with the location of $\sigma(i)$. For a basis tensor with m colour lines, the new gluon colour line and anti-colour line will have the indices $m+1$:

$$\begin{aligned} \boldsymbol{t}_{c_i} \left|\sigma^{(m)}\right\rangle &= \boldsymbol{t}_{c_i} \left|\sigma(1)\cdots\sigma(i)\cdots\sigma(m)\right\rangle \\ &= \left|\sigma(1)\cdots(m+1)\cdots\sigma(m),\sigma(i)\right\rangle . \end{aligned} \tag{3.26}$$

The second term simply inserts a colour line which flows from the newly formed anti-colour line. The operator therefore just appends the index of the new gluon at the end of the permutation list:

$$\begin{aligned} \boldsymbol{s} \left|\sigma^{(m)}\right\rangle &= \boldsymbol{s} \left|\sigma(1)\cdots\sigma(i)\cdots\sigma(m)\right\rangle \\ &= \left|\sigma(1)\cdots\sigma(i)\cdots\sigma(m),(m+1)\right\rangle . \end{aligned} \tag{3.27}$$

The colour charge operator for an anti-quark leg has a relative minus sign to that of the quark and the colour flows in the opposite direction:

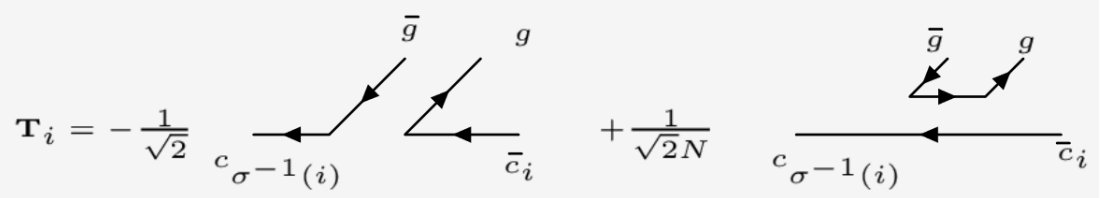

(3.28)

where $\sigma^{-1}(i)$ is the anti-permutation meaning the anti-colour line $\bar{c}_i$ flows to the colour line $c_{\sigma^{-1}(i)}$. The first term is defined to be the result of

$$\begin{aligned} \bar{\boldsymbol{t}}_{\bar{c}_i} |\sigma^{(m)}\rangle &= \bar{\boldsymbol{t}}_{\bar{c}_i} |1 \cdots i \cdots m\rangle \\ &= |1 \cdots (m+1) \cdots m, i\rangle \\ &= \boldsymbol{t}_{c_{\sigma^{-1}(i)}} |\sigma^{(m)}\rangle \\ \bar{\boldsymbol{t}}_{\bar{c}_{\sigma(i)}} |\sigma^{(m)}\rangle &= \boldsymbol{t}_{c_i} |\sigma^{(m)}\rangle \end{aligned} \tag{3.29}$$

where the last line makes the link between $\boldsymbol{t}_i$ and $\bar{\boldsymbol{t}}_i$ explicit: A gluon emission from any where along the colour flow has the same effect on the permutation. Redrawing the colour charge operator for a gluon leg from equation 3.8b such that no lines cross gives

$\mathbf{T}_i =$ 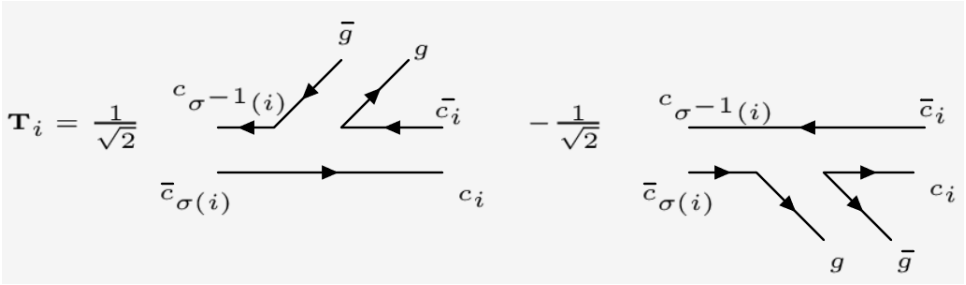 (3.30)

meaning the first term can be arrived at by applying the operator $\bar{\boldsymbol{t}}_{\bar{c}_i}$ and the second term requires $\boldsymbol{t}_{c_i}$.

The operators $\boldsymbol{t}_i$, $\bar{\boldsymbol{t}}_i$ and $\boldsymbol{s}$ are collectively know as colour line operators. Combined with the definitions in table 3.1 the general colour charge operator for leg i is then

$$\boldsymbol{T}_i = \lambda_i \boldsymbol{t}_{c_i} - \bar{\lambda}_i \bar{\boldsymbol{t}}_{\bar{c}_i} - \frac{1}{N}(\lambda_i - \bar{\lambda}_i)\boldsymbol{s}. \tag{3.31}$$

The hermitian conjugate $\boldsymbol{T}_j^\dagger$ has the same effect on $\langle\sigma|$. The quark leg is labelled a, the anti-quark leg is labelled b and the n^{th} gluon leg is labelled n. The gluon legs are composed of a colour line $c_n = n+1$ and an anti-colour line $\bar{c}_n = n+1$. The values of λ_i and $\bar{\lambda}_i$ are labelled such that the operator $\boldsymbol{T}_i$ (equation 3.31) reverts back to the colour charge operator for a quark, anti-quark or gluon depending on the leg being considered.

Leg i	c_i	$\bar{c}_i$	λ_i	$\bar{\lambda}_i$
Quark = a	1	0	$\frac{1}{\sqrt{2}}$	0
Anti-quark= b	0	1	0	$\frac{1}{\sqrt{2}}$
Gluon=n	$n+1$	$n+1$	$\frac{1}{\sqrt{2}}$	$\frac{1}{\sqrt{2}}$

TABLE 3.1: Colour Flow Basis book keeping.

To strip $\boldsymbol{T}_i$ and $\boldsymbol{T}_j^\dagger$ operators from the amplitude we then need to compute

$$\begin{aligned}
[\rho|\boldsymbol{A_n}|\sigma] &= [\rho|\boldsymbol{T}_i\boldsymbol{A_{n-1}}\boldsymbol{T}_j^\dagger|\sigma] \\
&= \sum_{\alpha\beta}[\rho|\boldsymbol{T}_i\,|\alpha\rangle\,[\alpha|\boldsymbol{H}|\beta]\,\langle\beta|\,\boldsymbol{T}_j^\dagger|\sigma] \\
&= \sum_{\alpha\beta}[\alpha|\boldsymbol{H}|\beta][\rho\,|\alpha'\rangle\,\boldsymbol{C}^\alpha_{T_i}C^\beta_{T_j}\,\langle\beta'|\,\sigma] \\
&= \sum_{\alpha\beta}[\alpha|\boldsymbol{H}|\beta]\delta_{\rho\alpha'}\delta_{\beta'\sigma}\boldsymbol{C}^\alpha_L\boldsymbol{C}^\beta_R
\end{aligned} \tag{3.32}$$

Considering just the amplitude evolution we have

$$\begin{aligned}
[\rho|\boldsymbol{T}_i\,|\alpha\rangle &= \lambda_i[\rho|\boldsymbol{t}_{c_i}\,|\alpha\rangle - \bar{\lambda}_i[\rho|\bar{\boldsymbol{t}}_{\bar{c}_i}\,|\alpha\rangle - \frac{1}{N}(\lambda_i-\bar{\lambda}_i)[\rho|\boldsymbol{s}\,|\alpha\rangle \\
&= \delta_{\rho\alpha'}\lambda_i - \delta_{\rho\alpha''}\bar{\lambda}_i - \frac{1}{N}(\lambda_i-\bar{\lambda}_i)\delta_{\rho\alpha'''}
\end{aligned} \tag{3.33}$$

meaning $\boldsymbol{T}_i$ causes three distinct new colour flows to be generated, α', α'' and α'''. All three involve the addition of the lines c_n and $\bar{c}_n$. In α', c_i is set to be the destination of the newly added anti-colour line hence we have a factor of $\delta_{c_i\rho^{-1}(n)}$ to impose this colour flow on the basis tensor ρ. In α', $\bar{c}_i$ is set to be the origin of the newly added colour line hence we have a factor of $\delta_{\bar{c}_i\rho(n)}$. Finally, in α''', c_i and $\bar{c}_i$ are unaltered and c_n flows from $\bar{c}_n$ meaning a factor of $\delta_{c_n\rho^{-1}(n)}$. The rest of the permutation of α is unchanged. An additional Kronecker delta must be applied to each of the terms to impose this. This is given by $\delta_{\rho/n,\alpha}$ which sets the permutation ρ, with the n^{th} lines removed and the resulting gap stitched, equivalent to the original α. Hence, the matrix elements for $\boldsymbol{T}_i$ are

$$[\rho|\boldsymbol{T}_i\,|\alpha\rangle = \delta_{\rho/n,\alpha}\left(\lambda_i\delta_{c_i\rho^{-1}(n)} - \bar{\lambda}_i\delta_{\bar{c}_i\rho(n)} - \frac{1}{N}(\lambda_i - \bar{\lambda}_i)\delta_{c_n\rho^{-1}(n)}\right). \tag{3.34}$$

Similarly,

$$\begin{aligned}\langle\sigma|\,\boldsymbol{T}_j|\beta] &= \lambda_j\,\langle\sigma|\,\boldsymbol{t}_{c_j}|\beta] - \bar{\lambda}_j\,\langle\sigma|\,\bar{\boldsymbol{t}}_{\bar{c}_j}|\beta] - \frac{1}{N}(\lambda_j - \bar{\lambda}_j)\,\langle\sigma|\,\boldsymbol{s}|\beta] \\ &= \left(\lambda_j\delta_{c_j\sigma^{-1}(n)} - \bar{\lambda}_j\delta_{\bar{c}_j\sigma(n)} - \frac{1}{N}(\lambda_j - \bar{\lambda}_j)\delta_{c_n\sigma^{-1}(n)}\right)\delta_{\sigma/n,\beta}.\end{aligned} \tag{3.35}$$

3.5 Virtual Corrections

The virtual corrections are marked by a dot product of colour charge operators

$$\boldsymbol{T}_i \cdot \boldsymbol{T}_j = \boldsymbol{T}_i^{(g)}\boldsymbol{T}_j^{(g)} \tag{3.36}$$

which has the effect of $\boldsymbol{T}_i$ acting on leg i to insert a pair of colour/anti-colour lines and $\boldsymbol{T}_j$ doing the same to leg j. The dot product indicates that we should join the newly formed gluon colour lines at leg i with those at j. This is a consequence of the two operators sharing a gluon index g.

The expansion of the dot product requires:

$$\boldsymbol{s}\cdot\boldsymbol{s} = N\boldsymbol{I} \tag{3.37a}$$

$$\boldsymbol{t}_{c_i}\cdot\boldsymbol{s} = \boldsymbol{I} \tag{3.37b}$$

$$\bar{\boldsymbol{t}}_{\bar{c}_i}\cdot\boldsymbol{s} = \boldsymbol{I} \tag{3.37c}$$

$$\boldsymbol{t}_{c_i}\cdot\bar{\boldsymbol{t}}_{\bar{c}_j} = \{\bar{c}_j\bar{c}_{\sigma(i)}\} = \{c_ic_{\sigma^{-1}(j)}\} \tag{3.37d}$$

$$\bar{\boldsymbol{t}}_{\bar{c}_i}\cdot\bar{\boldsymbol{t}}_{\bar{c}_j} = \{\bar{c}_i\bar{c}_j\} = \{c_{\sigma^{-1}(i)}c_{\sigma^{-1}(j)}\} \tag{3.37e}$$

$$\boldsymbol{t}_{c_i}\cdot\boldsymbol{t}_{c_j} = \{c_ic_j\} = \{\bar{c}_{\sigma(i)}\bar{c}_{\sigma(j)}\} \tag{3.37f}$$

where elements in curly brackets correspond to a transposition in the colour flow. For example, $\{c_ic_j\}$ refers to the transposition of the colour lines i and j.

The matrix elements for the expansion of $\boldsymbol{T}_i \cdot \boldsymbol{T}_j$ are then given by:

$$\begin{aligned}\lambda_i \left(-\frac{1}{N}(\lambda_j - \bar{\lambda}_j)\right) [\tau|\boldsymbol{t}_{c_i} \cdot \boldsymbol{s}\,|\sigma\rangle + (i \leftrightarrow j) &= \lambda_i \left(-\frac{1}{N}(\lambda_j - \bar{\lambda}_j)\right) [\tau\,|\sigma\rangle + (i \leftrightarrow j) \\ &= \lambda_i \left(-\frac{1}{N}(\lambda_j - \bar{\lambda}_j)\right) \delta_{\tau\sigma} + (i \leftrightarrow j)\end{aligned} \tag{3.38a}$$

$$\begin{aligned}-\bar{\lambda}_i \left(-\frac{1}{N}(\lambda_j - \bar{\lambda}_j)\right) [\tau|\bar{\boldsymbol{t}}_{\bar{c}_i} \cdot \boldsymbol{s}\,|\sigma\rangle + (i \leftrightarrow j) &= -\bar{\lambda}_i \left(-\frac{1}{N}(\lambda_j - \bar{\lambda}_j)\right) [\tau\,|\sigma\rangle + (i \leftrightarrow j) \\ &= -\bar{\lambda}_i \left(-\frac{1}{N}(\lambda_j - \bar{\lambda}_j)\right) \delta_{\tau\sigma} + (i \leftrightarrow j)\end{aligned} \tag{3.38b}$$

$$\begin{aligned}\left(-\frac{1}{N}(\lambda_i - \bar{\lambda}_i)\right)\left(-\frac{1}{N}(\lambda_j - \bar{\lambda}_j)\right) [\tau|\boldsymbol{s} \cdot \boldsymbol{s}\,|\sigma\rangle &= \left(-\frac{1}{N}(\lambda_i - \bar{\lambda}_i)\right)\left(-\frac{1}{N}(\lambda_j - \bar{\lambda}_j)\right) N[\tau\,|\sigma\rangle \\ &= \frac{1}{N}(\lambda_i - \bar{\lambda}_i)(\lambda_j - \bar{\lambda}_j)\delta_{\tau\sigma}\end{aligned} \tag{3.38c}$$

$$\begin{aligned}&\frac{1}{N}(\lambda_i - \bar{\lambda}_i)(\lambda_j - \bar{\lambda}_j) + (-\bar{\lambda}_i \left(-\frac{1}{N}(\lambda_j - \bar{\lambda}_j)\right) + (i \leftrightarrow j)) + (\lambda_i \left(-\frac{1}{N}(\lambda_j - \bar{\lambda}_j)\right) + (i \leftrightarrow j)) \\ &= -\frac{1}{N}(\lambda_i - \bar{\lambda}_i)(\lambda_j - \bar{\lambda}_j)\end{aligned} \tag{3.38d}$$

where the last line is the sum of the coefficients of $\delta_{\tau\sigma}$. The dot product $\boldsymbol{t}_{c_i} \cdot \boldsymbol{t}_{c_j}$results in the transposition of the colour lines c_i and c_j. If τ differs from σ by more than one transposition, the transposed colour flow σ' will still be at least one transposition away from τ and $[\tau\,|\sigma'\rangle = \delta_{\tau\sigma'} = 0$. This is the case if τ matches σ exactly as the transposition will shift σ away from τ and $[\tau\,|\sigma'\rangle = \delta_{\tau\sigma'} = 0$. However, if τ differs from σ by the exact transposition that $\boldsymbol{t}_{c_i} \cdot \boldsymbol{t}_{c_j}$ causes then $[\tau\,|\sigma'\rangle = \delta_{\tau\sigma'} = 1$ as the dot product reverses the transposition. The matrix elements for $\boldsymbol{t}_{c_i} \cdot \boldsymbol{t}_{c_j}$must therefore given by a sum over transpositions of colour lines $\{ab\}$ between τ and σ to include each of these possibilities:

$$\begin{aligned}\lambda_i\lambda_j[\tau|\boldsymbol{t}_{c_i} \cdot \boldsymbol{t}_{c_j}\,|\sigma\rangle &= \lambda_i\lambda_j\delta_{\tau\sigma'} \\ &= \lambda_i\lambda_j \sum_{\{ab\}} \delta_{\tau_{(ab)}\sigma}(\delta_{(ab),(c_ic_j)}).\end{aligned} \tag{3.39}$$

The same logic is applied for the matrix elements of $\bar{\boldsymbol{t}}_{\bar{c}_i} \cdot \bar{\boldsymbol{t}}_{\bar{c}_j}$ except the transposition between τ and σ must match the transposition generated by $\bar{\boldsymbol{t}}_{\bar{c}_i} \cdot \bar{\boldsymbol{t}}_{\bar{c}_j}$, $\{c_{\sigma^{-1}(i)} c_{\sigma^{-1}(j)}\}$:

$$\begin{aligned} \lambda_i \lambda_j [\tau | \bar{\boldsymbol{t}}_{\bar{c}_i} \cdot \bar{\boldsymbol{t}}_{\bar{c}_j} | \sigma \rangle &= \bar{\lambda}_i \bar{\lambda}_j \delta_{\tau\sigma'} \\ &= \bar{\lambda}_i \bar{\lambda}_j \sum_{\{ab\}} \delta_{\tau_{(ab)}\sigma} (\delta_{(ab),(\sigma^{-1}(i)\sigma^{-1}(j))}) \end{aligned} \tag{3.40}$$

where I have used the simplified notation $\{\sigma^{-1}(i)\sigma^{-1}(j)\} \equiv \{c_{\sigma^{-1}(i)} c_{\sigma^{-1}(j)}\}$. Finally, $\boldsymbol{t}_{c_i} \cdot \bar{\boldsymbol{t}}_{\bar{c}_j}$ generates the transposition

$$\boldsymbol{t}_{c_i} \cdot \bar{\boldsymbol{t}}_{\bar{c}_j} = \{\bar{c}_j \bar{c}_{\sigma(i)}\} = \{c_i c_{\sigma^{-1}(j)}\} \tag{3.41}$$

which forms a closed loop if the legs i and j were colour connected in the original flow and as such we assign a factor of N. Colour connected refers to the cases where $i = \sigma^{-1}(j)$ meaning the colour line $\bar{c}_j$ flows to c_i. If the legs are not colour connected then the terms results in a transposition and the same argument as above is applied to arrive at

$$\begin{aligned} -\lambda_i \bar{\lambda}_j [\tau | \bar{\boldsymbol{t}}_{\bar{c}_i} \cdot \bar{\boldsymbol{t}}_{\bar{c}_j} | \sigma \rangle &= -\lambda_i \bar{\lambda}_j \delta_{\tau\sigma'} \\ &= -\lambda_i \bar{\lambda}_j N \delta_{\tau\sigma} \delta_{c_i \bar{c}_{\sigma^{-1}(j)}} - \lambda_i \bar{\lambda}_j \sum_{\{ab\}} \delta_{\tau_{(ab)}\sigma} (\delta_{(ab),(i\sigma^{-1}(j))}) \end{aligned} \tag{3.42}$$

The term $\boldsymbol{t}_{c_j} \cdot \bar{\boldsymbol{t}}_{\bar{c}_i}$ leads to the same result with $i \leftrightarrow j$.

Combining each of these terms gives the entire colour charge operator dot product to be

$$\begin{aligned} [\tau | \boldsymbol{T}_i \cdot \boldsymbol{T}_j | \sigma \rangle = -N \delta\tau\sigma \Bigg(& \lambda_i \bar{\lambda}_j \delta_{c_i \bar{c}_{\sigma^{-1}(j)}} + \lambda_j \bar{\lambda}_i \delta_{c_j \bar{c}_{\sigma^{-1}(i)}} + \frac{1}{N^2} (\lambda_i - \bar{\lambda}_i)(\lambda_j - \bar{\lambda}_j) \Bigg) \\ & \sum_{\{ab\}} \delta_{\tau_{(ab)}\sigma} \left(-\lambda_i \bar{\lambda}_j \delta_{(ab),(i\sigma^{-1}(j))} - \lambda_i \bar{\lambda}_j \delta_{(ab),(j\sigma^{-1}(i))} \right. \\ & \left. + \bar{\lambda}_i \bar{\lambda}_j \delta_{(ab),(\sigma^{-1}(i)\sigma^{-1}(j))} + \lambda_i \lambda_j \delta_{(ab),(ij)} \right). \end{aligned} \tag{3.43}$$

3.6 Using the Colour Flow Basis

Rules to generate these matrix elements were written into a Mathematica document by Matthew De Angelis [10]. I then expanded this document to calculate the emission functions as defined in chapter 2. The results are given in seen in table 3.2.

Emission Functions	
ϵ_0	N
$\epsilon_1^{(1)}$	$-\left(N^2-1\right)\omega_{ab}^1$
$\epsilon_2^{(1,2)}$	$\frac{\left(N^2-1\right)\omega_{ab}^1\left(N^2\left(\omega_{a1}^2+\omega_{b1}^2\right)-\omega_{ab}^2\right)}{N}$
$\epsilon_3^{(1,2,3)}$	$-\left(N^2-1\right)\omega_{ab}^1\left(N^2\left(\omega_{a1}^2\left(\omega_{a2}^3+\omega_{b1}^3+\omega_{1\ 2}^3\right)+\omega_{b1}^2\left(\omega_{a1}^3+\omega_{b2}^3+\omega_{1\ 2}^3\right)\right)\right)$ $+\frac{\left(N^2-1\right)\omega_{ab}^1\left(N^2\left(\omega_{a1}^2+\omega_{b1}^2\right)\omega_{ab}^3+\omega_{ab}^2\left(\left(N^2+1\right)\omega_{ab}^3-N^2\left(\omega_{a1}^3+\omega_{a2}^3+\omega_{b1}^3+\omega_{b2}^3\right)\right)\right)}{N^2}$
$f_0^{(k)}$	$\frac{\left(N^2-1\right)\omega_{ab}^k}{2N}$
$f_1^{(k)}$	$\frac{1}{2}N\left(\omega_{a1}^k+\omega_{b1}^k\right)-\frac{\omega_{ab}^k}{2N}$
$f_2^{(k)}$	$\frac{N^2\left(N^2\omega_{a1}^2\omega_{b1}^k+\omega_{a2}^k\left(N^2\omega_{a1}^2-\omega_{ab}^2\right)+\omega_{a1}^k\left(N^2\omega_{b1}^2-\omega_{ab}^2\right)\right)}{2N^3\left(\omega_{a1}^2+\omega_{b1}^2\right)-2N\omega_{ab}^2}$ $+\frac{\left(-\omega_{ab}^2{\omega_{b1}}^k-{\omega_{ab}}^2{\omega_{b2}}^k+N^2\omega_{a1}^2\omega_{1\ 2}^k+N^2\omega_{b1}^2\omega_{12}^k+N^2\omega_{b1}^2\omega_{b2}^k\right)+\omega_{ab}^k\left(\left(N^2+1\right)\omega_{ab}^2-N^2\left(\omega_{a1}^2+\omega_{b1}^2\right)\right)}{2N^3\left(\omega_{a1}^2+\omega_{b1}^2\right)-2N\omega_{ab}^2}$

TABLE 3.2: Emission Functions calculated using the Colour Flow Basis

Chapter 4

Gaps between Jets up to Third Order

This chapter will calculate the cross sections for the gaps between jets observable up to first, second and third order in $\frac{\alpha_s L}{\pi}$. The dependence on the collinear cut-off λ is shown to cancel exactly for the first order calculation whereas the second and third order calculations retain potential dependence on λ. I simplify the calculations as much as possible, ready to be numerically integrated to test for λ independence. At any point where I express an emission function (ϵ or f) in terms of colour factors and radiation functions ω_{ij}^k I have used table 3.2 from chapter 3.

4.1 Zero Reals

The cross-section for zero real emissions up to p^{th} order is

$$\Sigma_0^{(p)}(\mu) = \int d\sigma_0^{(p)} \tag{4.1}$$

which is the the subset of terms in

$$\mathrm{Tr}[\boldsymbol{V}_{\mu,Q}\boldsymbol{H}(Q)\boldsymbol{V}_{\mu,Q}^{\dagger}] \tag{4.2}$$

which are p^{th} order in $\frac{\alpha_s L}{\pi}$. As shown in Chapter 3

$$\boldsymbol{T}_a \cdot \boldsymbol{T}_b = -C_F \boldsymbol{I} \tag{4.3}$$

which makes the Sudakov abelian. The exponent of the Sudakov and conjugate Sudakov can be combined and then extracted from the trace which leads to the cancellation of the absorptive (Coulomb) term

$$\begin{aligned}
\mathrm{Tr}[\boldsymbol{V}_{\mu,Q}\boldsymbol{H}(Q)\boldsymbol{V}_{\mu,Q}^{\dagger}] &= \mathrm{Tr}[\boldsymbol{V}_{\mu,Q}^{\dagger}\boldsymbol{V}_{\mu,Q}\boldsymbol{H}] \\
&= \mathrm{Tr}[\exp\left[\boldsymbol{I}_0 + \boldsymbol{I}_0^{\dagger}\right]\boldsymbol{H}] \\
&= \mathrm{Tr}[\exp\left[\boldsymbol{R}_0 + \boldsymbol{R}_0^{\dagger} + \boldsymbol{A}_0^{\dagger} + \boldsymbol{A}_0\right]\boldsymbol{H}] \\
&= \mathrm{Tr}[\exp\left[2\boldsymbol{R}_0 - \boldsymbol{A}_0 + \boldsymbol{A}_0\right]\boldsymbol{H}] \\
&= \mathrm{Tr}[\exp\left[2\boldsymbol{R}_0\right]\boldsymbol{H}] \\
&= \mathrm{Tr}[\exp\left[-2\frac{\alpha_s}{\pi}t_0^{'}\bar{\boldsymbol{F}}_0^{(k)}\right]\boldsymbol{H}] \\
&= \exp\left[-2\frac{\alpha_s}{\pi}t_0^{'}\bar{f}_0^{(k)}\right]\mathrm{Tr}[\boldsymbol{H}]
\end{aligned} \tag{4.4}$$

This gives

$$\Sigma_0^{(p)}(\mu) = \left(\frac{-\alpha_s}{\pi}\right)^p \epsilon_0 \frac{\left(2t_0^{'}\bar{f}_0^{(k)}\right)^p}{p!} \tag{4.5}$$

where

$$t_0^{'} = t_0 - \ln\frac{\mu}{\mu} = \ln\frac{Q}{\mu} = L \tag{4.6}$$

resulting in

$$\Sigma_0^{(p)}(\mu) = \left(\frac{-\alpha_s L}{\pi}\right)^p \epsilon_0 \frac{\left(2\bar{f}_0^{(k)}\right)^p}{p!}. \tag{4.7}$$

4.2 One Real

In chapter 3 the colour matrices for the Sudakov between the first and second emission were shown to be

$$\boldsymbol{T}_a \cdot \boldsymbol{T}_b = \left(\frac{C_A}{2} - C_F\right)\boldsymbol{I} \tag{4.8a}$$

$$\boldsymbol{T}_a \cdot \boldsymbol{T}_1 = -\frac{C_A}{2}\boldsymbol{I} \tag{4.8b}$$

$$\boldsymbol{T}_b \cdot \boldsymbol{T}_1 = -\frac{C_A}{2}\boldsymbol{I} \tag{4.8c}$$

meaning the exponent of the second Sudakov is also abelian. The first and second pair of Sudakovs can both be extracted from the trace and the absorptive terms from

both can be cancelled

$$\begin{aligned}\mathrm{Tr}[\boldsymbol{V}_{\mu,E_1}\boldsymbol{D}_1^{\nu}\boldsymbol{V}_{E_1,Q}\boldsymbol{H}(Q)\boldsymbol{V}_{E_1,Q}^{\dagger}\boldsymbol{D}_{1\nu}^{\dagger}\boldsymbol{V}_{\mu,E_1}^{\dagger}] &= \mathrm{Tr}[\exp[\boldsymbol{I}_0+\boldsymbol{I}_1+\boldsymbol{I}_0^{\dagger}+\boldsymbol{I}_1^{\dagger}]\boldsymbol{D}_1^{\nu}\boldsymbol{H}(Q)\boldsymbol{D}_{1\nu}^{\dagger}]\\ &= \mathrm{Tr}[\exp[2\boldsymbol{R}_0+2\boldsymbol{R}_1]\boldsymbol{D}_1^{\nu}\boldsymbol{H}(Q)\boldsymbol{D}_{1\nu}^{\dagger}]\\ &= \exp\left(\frac{-2\alpha_s}{\pi}\left(t_0^{'}\bar{f}_0^{(k)}+t_1^{'}\bar{f}_1^{(k)}\right)\right)\mathrm{Tr}[\boldsymbol{D}_1^{\nu}\boldsymbol{H}(Q)\boldsymbol{D}_{1\nu}^{\dagger}]\end{aligned} \tag{4.9}$$

which gives the cross section up to all orders as

$$\begin{aligned}\Sigma_1(\mu) &= \int d\sigma_1 u_1(k_1)\\ &= \left(\frac{-\alpha_s}{\pi}\right)\int_0^{t_0} dt_1\ddot{\epsilon}_1^{(1)}\exp\left(\frac{-2\alpha_s}{\pi}\left(t_0^{'}\bar{f}_0^{(k)}+t_1^{'}\bar{f}_1^{(k)}\right)\right)\\ &= \left(\frac{-\alpha_s}{\pi}\right)\int_0^{t_0} dt_1\ddot{\epsilon}_1^{(1)}\left[\sum_{p=0}^{\infty}\left(\frac{-2\alpha_s}{\pi}\right)^p\frac{\left(t_0^{'}\bar{f}_0^{(k)}+t_1^{'}\bar{f}_1^{(k)}\right)^p}{p!}\right]\\ &= \left(\frac{-\alpha_s}{\pi}\right)\int_0^{t_0} dt_1\ddot{\epsilon}_1^{(1)}\left[\sum_{p=1}^{\infty}\left(\frac{-2\alpha_s}{\pi}\right)^{p-1}\frac{\left(t_0^{'}\bar{f}_0^{(k)}+t_1^{'}\bar{f}_1^{(k)}\right)^{p-1}}{(p-1)!}\right]\end{aligned} \tag{4.10}$$

Terms of order p can then be extracted corresponding to cross section contributions of 1 real emissions and $p-1$ virtual corrections (note $t_0 \equiv L = \ln\frac{Q}{\mu}$):

$$\begin{aligned}\Sigma_1^{(1)}(\mu) &= \left(\frac{-\alpha_s}{\pi}\right)\int_0^{t_0} dt_1\ddot{\epsilon}_1^{(1)}\left[\left(\frac{-\alpha_s}{\pi}\right)^{(1-1)}\frac{\left(2t_0^{'}\bar{f}_0^{(k)}+2t_1^{'}\bar{f}_1^{(k)}\right)^{(1-1)}}{(1-1)!}\right]\\ &= \left(\frac{-\alpha_s L}{\pi}\right)\ddot{\epsilon}_1^{(1)}\end{aligned} \tag{4.11}$$

$$\begin{aligned}\Sigma_1^{(2)}(\mu) &= \left(\frac{-\alpha_s}{\pi}\right)\int_0^{t_0} dt_1\ddot{\epsilon}_1^{(1)}\left[\left(\frac{-\alpha_s}{\pi}\right)^{(2-1)}\frac{\left(2t_0^{'}\bar{f}_0^{(2)}+2t_1^{'}\bar{f}_1^{(2)}\right)^{(2-1)}}{(2-1)!}\right]\\ &= \left(\frac{-\alpha_s}{\pi}\right)\int_0^{t_0} dt_1\ddot{\epsilon}_1^{(1)}\left[\left(\frac{-\alpha_s}{\pi}\right)2\left(t_0^{'}\bar{f}_0^{(2)}+t_1^{'}\bar{f}_1^{(2)}\right)\right]\\ &= \left(\frac{-\alpha_s}{\pi}\right)\int_0^{t_0} dt_1\ddot{\epsilon}_1^{(1)}\left[\left(\frac{-\alpha_s}{\pi}\right)2\left((t_0-t_1)\bar{f}_0^{(2)}+t_1\bar{f}_1^{(2)}\right)\right]\\ &= \left(\frac{-\alpha_s}{\pi}\right)\ddot{\epsilon}_1^{(1)}\left[\left(\frac{-\alpha_s}{\pi}\right)2\left((t_0^2-\frac{t_0^2}{2})\bar{f}_0^{(2)}+\frac{t_0^2}{2}\bar{f}_1^{(2)}\right)\right]\\ &= \left(\frac{-\alpha_s L}{\pi}\right)^2\ddot{\epsilon}_1^{(1)}\left[\left(\bar{f}_0^{(2)}+\bar{f}_1^{(2)}\right)\right]\end{aligned} \tag{4.12}$$

$$\begin{aligned}\Sigma_1^{(3)}(\mu) &= \left(\frac{-\alpha_s}{\pi}\right)\int_0^{t_0} dt_1 \ddot{\epsilon}_1^{(1)}\left[\left(\frac{-\alpha_s}{\pi}\right)^{(3-1)}\frac{\left(2\acute{t_0}\bar{f}_0^{(k)}+2\acute{t_1}\bar{f}_1^{(k)}\right)^{(3-1)}}{(3-1)!}\right]\\ &= \left(\frac{-\alpha_s}{\pi}\right)\int_0^{t_0} dt_1 \ddot{\epsilon}_1^{(1)}\left[\left(\frac{-\alpha_s}{\pi}\right)^{2}\frac{2^2}{(2)!}\left(\acute{t_0}\bar{f}_0^{(2)}+\acute{t_1}\bar{f}_1^{(2)}\right)\left(\acute{t_0}\bar{f}_0^{(3)}+\acute{t_1}\bar{f}_1^{(3)}\right)\right]\\ &= \left(\frac{-\alpha_s L}{\pi}\right)^3\frac{2}{3}\ddot{\epsilon}_1^{(1)}\left(\bar{f}_0^{(2)}\bar{f}_0^{(3)}+\bar{f}_0^{(2)}\bar{f}_1^{(3)}+\bar{f}_1^{(2)}\bar{f}_1^{(3)}\right)\end{aligned} \tag{4.13}$$

The steps below make the calculation more explicit

$$\begin{aligned}\int_0^{t_0} dt_1\left(\acute{t_0}\bar{f}_0^{(2)}+\acute{t_1}\bar{f}_1^{(2)}\right)\left(\acute{t_0}\bar{f}_0^{(3)}+\acute{t_1}\bar{f}_1^{(3)}\right) &= \int_0^{t_0} dt_1\Big[(t_0^2-2t_0t_1+t_1^2)\bar{f}_0^{(2)}\bar{f}_0^{(3)}+\\ &\quad t_1(t_0-t_1)\bar{f}_0^{(2)}\bar{f}_1^{(3)}\\ &\quad +t_1(t_0-t_1)\bar{f}_1^{(2)}\bar{f}_0^{(3)}+t_1^2\bar{f}_1^{(2)}\bar{f}_1^{(3)}\Big]\\ &= \int_0^{t_0} dt_1\Big[(t_0^2-2t_0t_1+t_1^2)\bar{f}_0^{(2)}\bar{f}_0^{(3)}+\\ &\quad 2t_1(t_0-t_1)\bar{f}_1^{(2)}\bar{f}_0^{(3)}+t_1^2\bar{f}_1^{(2)}\bar{f}_1^{(3)}\Big]\\ &= L^3\left(\frac{1}{3}\bar{f}_0^{(2)}\bar{f}_0^{(3)}+\frac{1}{3}\bar{f}_1^{(2)}\bar{f}_0^{(3)}+\frac{1}{3}\bar{f}_1^{(2)}\bar{f}_1^{(3)}\right)\end{aligned} \tag{4.14}$$

where I have used in the middle line the fact that the gluon labels for virtual f emission functions can be switched i.e.the order in which they are integrated is arbitrary (see 2.75).

4.3 Two Reals

The trace for 2 real emissions is

$$\mathrm{Tr}\left(\boldsymbol{V}_{E_3=\mu,E_2}\boldsymbol{D}_2^{\mu}\boldsymbol{V}_{E_2,E_1}\boldsymbol{D}_1^{\nu}\boldsymbol{V}_{E_1,Q}\boldsymbol{H}(Q)\boldsymbol{V}_{E_1,Q}^{\dagger}\boldsymbol{D}_{1\nu}^{\dagger}\boldsymbol{V}_{E_2,E_1}^{\dagger}\boldsymbol{D}_{2\mu}^{\dagger}\boldsymbol{V}_{E_3=\mu,E_2}^{\dagger}\right) \tag{4.15}$$

The colour factors for the third Sudakov are not abelian however the outermost Sudakovs can always be combined due to the cyclicity of the trace and the remaining

two pairs can be commuted which leads to the cancellation of the absorptive terms

$$\begin{aligned}
&\mathrm{Tr}\left(\boldsymbol{V}_{E_3=\mu,E_2}\boldsymbol{D}_2^{\mu}\boldsymbol{V}_{E_2,E_1}\boldsymbol{D}_1^{\nu}\boldsymbol{V}_{E_1,Q}\boldsymbol{H}(Q)\boldsymbol{V}_{E_1,Q}^{\dagger}\boldsymbol{D}_{1\nu}^{\dagger}\boldsymbol{V}_{E_2,E_1}^{\dagger}\boldsymbol{D}_{2\mu}^{\dagger}\boldsymbol{V}_{E_3=\mu,E_2}^{\dagger}\right)\\
&=\mathrm{Tr}\left(\boldsymbol{V}_{E_3=\mu,E_2}^{\dagger}\boldsymbol{V}_{E_3=\mu,E_2}\boldsymbol{V}_{E_2,E_1}V_{E_1,Q}\boldsymbol{V}_{E_1,Q}^{\dagger}\boldsymbol{V}_{E_2,E_1}^{\dagger}\boldsymbol{D}_2^{\mu}\boldsymbol{D}_1^{\nu}\boldsymbol{H}(Q)\boldsymbol{D}_{1\nu}^{\dagger}\boldsymbol{D}_{2\mu}^{\dagger}\right)\\
&=\mathrm{Tr}\left(\exp\left(\frac{-2\alpha_s}{\pi}\left(t_0^{'}\bar{\boldsymbol{F}}_0^{(k)}+t_1^{'}\bar{\boldsymbol{F}}_1^{(k)}+t_2^{'}\bar{\boldsymbol{F}}_2^{(k)}\right)\right)\boldsymbol{D}_2^{\mu}\boldsymbol{D}_1^{\nu}\boldsymbol{H}(Q)\boldsymbol{D}_{1\nu}^{\dagger}\boldsymbol{D}_{2\mu}^{\dagger}\right)\\
&=\mathrm{Tr}\left(\left[\sum_{p=0}^{\infty}\left(\frac{-2\alpha_s}{\pi}\right)^p\frac{\left(t_0^{'}\bar{\boldsymbol{F}}_0^{(k)}+t_1^{'}\bar{\boldsymbol{F}}_1^{(k)}+t_2^{'}\bar{\boldsymbol{F}}_2^{(k)}\right)^p}{p!}\right]\boldsymbol{D}_2^{\mu}\boldsymbol{D}_1^{\nu}\boldsymbol{H}(Q)\boldsymbol{D}_{1\nu}^{\dagger}\boldsymbol{D}_{2\mu}^{\dagger}\right)
\end{aligned}\tag{4.16}$$

where combining the exponents of the Sudakovs and conjugate Sudakovs has lead to the cancellation of the absorptive terms as it did for the case of zero and one real emission. However, the expansion must remain in the trace as $\boldsymbol{F}_2^{(k)}$ is non-abelian, this gives

$$\begin{aligned}
\Sigma_2(\mu)=&\left(\frac{-\alpha_s}{\pi}\right)^2\int_0^{t_0}dt_1\int_0^{t_1}dt_2\\
&\mathrm{Tr}\left(\left[\sum_{p=2}^{\infty}\left(\frac{-2\alpha_s}{\pi}\right)^{p-2}\frac{\left(t_0^{'}\bar{\boldsymbol{F}}_0^{(k)}+t_1^{'}\bar{\boldsymbol{F}}_1^{(k)}+t_2^{'}\bar{\boldsymbol{F}}_2^{(k)}\right)^{p-2}}{(p-2)!}\right]\boldsymbol{D}_2^{\mu}\boldsymbol{D}_1^{\nu}\boldsymbol{H}(Q)\boldsymbol{D}_{1\nu}^{\dagger}\boldsymbol{D}_{2\mu}^{\dagger}\right)
\end{aligned}\tag{4.17}$$

Terms of order p can then be extracted corresponding to cross sections for 2 real emissions and $p-2$ virtual corrections:

$$\begin{aligned}
\Sigma_2^{(2)}(\mu)=&\left(\frac{-\alpha_s}{\pi}\right)^2\int_0^{t_0}dt_1\int_0^{t_1}dt_2\\
&\mathrm{Tr}\left(\left[\left(\frac{-2\alpha_s}{\pi}\right)^{2-2}\frac{\left(t_0^{'}\bar{\boldsymbol{F}}_0^{(k)}+t_1^{'}\bar{\boldsymbol{F}}_1^{(k)}+t_2^{'}\bar{\boldsymbol{F}}_2^{(k)}\right)^{2-2}}{(2-2)!}\right]\ddot{\boldsymbol{D}}_2^{\mu}\ddot{\boldsymbol{D}}_1^{\nu}\boldsymbol{H}(Q)\ddot{\boldsymbol{D}}_{1\nu}^{\dagger}\ddot{\boldsymbol{D}}_{2\mu}^{\dagger}\right)\\
&=\left(\frac{-\alpha_s}{\pi}\right)^2\int_0^{t_0}dt_1t_1\mathrm{Tr}\left(\ddot{\boldsymbol{D}}_2^{\mu}\ddot{\boldsymbol{D}}_1^{\nu}\boldsymbol{H}(Q)\ddot{\boldsymbol{D}}_{1\nu}^{\dagger}\ddot{\boldsymbol{D}}_{2\mu}^{\dagger}\right)\\
&=\left(\frac{-\alpha_sL}{\pi}\right)^2\frac{1}{2}\ddot{\epsilon}_2^{(1,2)}
\end{aligned}\tag{4.18}$$

$$
\begin{aligned}
\Sigma_2^{(3)}(\mu) = & \left(\frac{-\alpha_s}{\pi}\right)^2 \int_0^{t_0} dt_1 \int_0^{t_1} dt_2 \\
& \mathrm{Tr}\left(\left[\left(\frac{-2\alpha_s}{\pi}\right)^{3-2} \frac{\left(t_0^{'}\bar{F}_0^{(3)} + t_1^{'}\bar{F}_1^{(3)} + t_2^{'}\bar{F}_2^{(3)}\right)^{3-2}}{(3-2)!}\right] \ddot{\boldsymbol{D}}_2^{\mu}\ddot{\boldsymbol{D}}_1^{\nu}\boldsymbol{H}(Q)\ddot{\boldsymbol{D}}_{1\nu}^{\dagger}\ddot{\boldsymbol{D}}_{2\mu}^{\dagger}\right) \\
= & \left(\frac{-\alpha_s}{\pi}\right)^3 \int_0^{t_0} dt_1 \int_0^{t_1} dt_2 2\mathrm{Tr}\left(\left[t_0^{'}\bar{F}_0^{(3)} + t_1^{'}\bar{F}_1^{(3)} + t_2^{'}\bar{F}_2^{(3)}\right] \ddot{\boldsymbol{D}}_2^{\mu}\ddot{\boldsymbol{D}}_1^{\nu}\boldsymbol{H}(Q)\ddot{\boldsymbol{D}}_{1\nu}^{\dagger}\ddot{\boldsymbol{D}}_{2\mu}^{\dagger}\right) \\
= & \left(\frac{-\alpha_s}{\pi}\right)^3 \int_0^{t_0} dt_1 \int_0^{t_1} dt_2 2\mathrm{Tr}\left(\ddot{\boldsymbol{D}}_2^{\mu}\ddot{\boldsymbol{D}}_1^{\nu}\boldsymbol{H}(Q)\ddot{\boldsymbol{D}}_{1\nu}^{\dagger}\ddot{\boldsymbol{D}}_{2\mu}^{\dagger}\right)\left[t_0^{'}\bar{f}_0^{(3)} + t_1^{'}\bar{f}_1^{(3)} + t_2^{'}\bar{f}_2^{(3)}\right] \\
= & \left(\frac{-\alpha_s}{\pi}\right)^3 \int_0^{t_0} dt_1 \int_0^{t_1} dt_2 2\ddot{\epsilon}_2^{(1,2)}\left[t_0^{'}\bar{f}_0^{(3)} + t_1^{'}\bar{f}_1^{(3)} + t_2^{'}\bar{f}_2^{(3)}\right] \\
= & \left(\frac{-\alpha_s}{\pi}\right)^3 \int_0^{t_0} dt_1 \int_0^{t_1} dt_2 \ddot{\epsilon}_2^{(1,2)}\left[(t_0 - t_1)\bar{f}_0^{(3)} + (t_1 - t_2)\bar{f}_1^{(3)} + t_2\bar{f}_2^{(3)}\right] \\
= & \left(\frac{-\alpha_s}{\pi}\right)^3 \int_0^{t_0} dt_1 2\ddot{\epsilon}_2^{(1,2)}\left[(t_0 t_1 - t_1^2)\bar{f}_0^{(3)} + (t_1^2 - \frac{t_1^2}{2})\bar{f}_1^{(3)} + \frac{t_1^2}{2}\bar{f}_2^{(3)}\right] \\
= & \left(\frac{-\alpha_s}{\pi}\right)^3 2\ddot{\epsilon}_2\left[(\frac{t_0^3}{2} - \frac{t_0^3}{3})\bar{f}_0^{(3)} + \frac{t_0^3}{3\cdot 2}\bar{f}_1^{(3)} + \frac{t_0^3}{3\cdot 2}\bar{f}_2^{(3)}\right] \\
= & \left(\frac{-\alpha_s L}{\pi}\right)^3 2\ddot{\epsilon}_2^{(1,2)}\left[\frac{1}{3\cdot 2}\bar{f}_0^{(3)} + \frac{1}{3\cdot 2}\bar{f}_1^{(3)} + \frac{1}{3\cdot 2}\bar{f}_2^{(3)}\right] \\
= & \left(\frac{-\alpha_s L}{\pi}\right)^3 \ddot{\epsilon}_2^{(1,2)}\left[\frac{1}{3}\bar{f}_0^{(3)} + \frac{1}{3}\bar{f}_1^{(3)} + \frac{1}{3}\bar{f}_2^{(3)}\right]
\end{aligned}
\tag{4.19}
$$

where I have used

$$
\bar{f}_2^{(k)} \equiv \frac{\mathrm{Tr}(\bar{\boldsymbol{F}}_2^{(k)}\boldsymbol{D}_2^{\mu}\boldsymbol{D}_1^{\nu}\boldsymbol{H}(Q)\boldsymbol{D}_{1,\nu}^{\dagger}\boldsymbol{D}_{2,\mu}^{\dagger})}{\epsilon_2} \tag{4.20}
$$

from Chapter 2.

4.4 Three Reals

For the third order calculation, expanding the Sudakovs in the 3 reals trace is not necessary. The required contribution is

$$\begin{aligned}\Sigma_3^{(3)}(\mu) &= \left(\frac{-\alpha_s}{\pi}\right)^3 \int_0^{t_0} dt_1 \int_0^{t_1} dt_2 \int_0^{t_2} dt_3 \mathrm{Tr}\left(\ddot{\boldsymbol{D}}_3^{\rho}\ddot{\boldsymbol{D}}_2^{\mu}\ddot{\boldsymbol{D}}_1^{\nu}\boldsymbol{H}(Q)\ddot{\boldsymbol{D}}_{1\nu}^{\dagger}\ddot{\boldsymbol{D}}_{2\mu}^{\dagger}\ddot{\boldsymbol{D}}_{3\rho}^{\dagger}\right) \\ &= \left(\frac{-\alpha_s}{\pi}\right)^3 \int_0^{t_0} dt_1 \int_0^{t_1} dt_2 \int_0^{t_2} dt_3 \ddot{\epsilon}_3^{(1,2,3)} \\ &= \left(\frac{-\alpha_s L}{\pi}\right)^3 \frac{1}{3\cdot 2}\ddot{\epsilon}_3^{(1,2,3)}.\end{aligned} \tag{4.21}$$

4.5 Gaps between Jets up to First Order

The gaps between jets observable up to 1^{st} order is

$$\begin{aligned}\Sigma^{(1)}(\mu) &= \Sigma_0^{(1)}(\mu) + \Sigma_1^{(1)}(\mu) \\ &= \left(\frac{-\alpha_s L}{\pi}\right)\left[\epsilon_0 \frac{\left(2\bar{f}_0^{(k)}\right)^1}{1!} + \ddot{\epsilon}_1^{(1)}\right] \\ &= \left(\frac{-\alpha_s L}{\pi}\right) 2\epsilon_0 \left[\bar{f}_0^{(1)} - \ddot{f}_0^{(1)}\right] \\ &= \left(\frac{-\alpha_s L}{\pi}\right) 2\epsilon_0 \dot{f}_0^{(1)} \\ &= \left(\frac{-\alpha_s L}{\pi}\right) \int_{-c}^{c} \frac{dx_1}{2} \int_0^{2\pi} \frac{d\phi_1}{2\pi} 2C_A(C_F\omega_{ab}^1\Theta_{cut}) \\ &= \left(\frac{-\alpha_s L}{\pi}\right) \int_0^{c} dx_1 2C_A C_F \omega_{ab}^1\end{aligned} \tag{4.22}$$

where the Heaviside function cuts away the collinear poles at n_a and n_b (see equation 2.45). The 3-vector parts of these point along the forward $x_1 = 1$ and backward $x_1 = -1$ azimuthal axes meaning the integral region of $x_1 = -c$ to $x_1 = c = cos(\alpha)$ does not include the poles and the integral is automatically λ independent. I have also used the fact that

$$\omega_{ab}^1 = \frac{n_a \cdot n_b}{n_a \cdot n_1 n_b \cdot n_1} = \frac{2}{1 - x_1^2} \tag{4.23}$$

meaning the integral has no azimuthal dependence and is symmetric about $x_1 = 0$.

4.6 Gaps between Jets up to Second Order

The gaps between jets observable up to 2^{nd} order is

$$\begin{aligned}\Sigma^{(2)}(\mu) &= \Sigma_0^{(2)}(\mu) + \Sigma_1^{(2)}(\mu) + \Sigma_2^{(2)}(\mu) \\ &= \left(\frac{-\alpha_s L}{\pi}\right)^2 \left[\epsilon_0 \frac{\left(2\bar{f}_0^{(k)}\right)^2}{2!} + \ddot{\epsilon}_1^{(1)}\left(\bar{f}_0^{(2)} + \bar{f}_1^{(2)}\right) + \frac{1}{2}\ddot{\epsilon}_2^{(1,2)}\right] \\ &= \left(\frac{-\alpha_s L}{\pi}\right)^2 \left[-\left(-2\epsilon_0 \bar{f}_0^{(1)}\right)\bar{f}_0^{(2)} + \ddot{\epsilon}_1^{(1)}\left(\bar{f}_0^{(2)} + \bar{f}_1^{(2)}\right) + \frac{1}{2}\ddot{\epsilon}_2^{(1,2)}\right] \\ &= \left(\frac{-\alpha_s L}{\pi}\right)^2 \left[-(\bar{\epsilon}_1^{(1)})\bar{f}_0 + \ddot{\epsilon}_1^{(1)}\left(\bar{f}_0^{(2)} + \bar{f}_1^{(2)}\right) + \frac{1}{2}\left(-2\ddot{\epsilon}_1^{(1)}\ddot{f}_1^{(2)}\right)\right].\end{aligned} \tag{4.24}$$

From equation 2.54

$$\begin{aligned}\dddot{\epsilon}_1 \bar{f}_1 - \ddot{\epsilon}_1 \ddot{\bar{f}}_1 &= \dddot{\epsilon}_1 \dot{f}_1 \\ (-\bar{\epsilon}_1)\bar{f}_0 + \ddot{\epsilon}_1 \bar{f}_0 &= -\dot{\epsilon}_1 \bar{f}_0\end{aligned} \tag{4.25}$$

and from equation 2.76

$$\begin{aligned}\dot{\epsilon}_1 \bar{f}_0 &= -2\epsilon_0 \dot{f}_0 \bar{f}_0 \\ &= -2\epsilon_0 \bar{f}_0 \dot{f}_0 \\ &= \bar{\epsilon}_1 \dot{f}_0\end{aligned} \tag{4.26}$$

which give

$$\begin{aligned}\Sigma^{(2)}(\mu) &= \left(\frac{-\alpha_s L}{\pi}\right)^2 \left[(-\bar{\epsilon}_1^{(1)})\bar{f}_0^{(2)} + \ddot{\epsilon}_1^{(1)}\left(\bar{f}_0^{(2)} + \bar{f}_1^{(2)}\right) + \frac{1}{2}\left(-2\ddot{\epsilon}_1^{(1)}\ddot{f}_1^{(2)}\right)\right] \\ &= \left(\frac{-\alpha_s L}{\pi}\right)^2 \left[\ddot{\epsilon}_1^{(1)}\dot{f}_1^{(2)} - \dot{\epsilon}_1^{(1)}\bar{f}_0^{(2)}\right] \\ &= \left(\frac{-\alpha_s L}{\pi}\right)^2 \left[\ddot{\epsilon}_1^{(1)}\dot{f}_1^{(2)} - \bar{\epsilon}_1^{(1)}\dot{f}_0^{(2)}\right] \\ &= \left(\frac{-\alpha_s L}{\pi}\right)^2 \left[\ddot{\epsilon}_1^{(1)}\dot{f}_1^{(2)} - \left(\ddot{\epsilon}_1^{(1)} + \dot{\epsilon}_1^{(1)}\right)\dot{f}_0^{(2)}\right] \\ &= \left(\frac{-\alpha_s L}{\pi}\right)^2 \left[\ddot{\epsilon}_1^{(1)}\left(\dot{f}_1^{(2)} - \dot{f}_0^{(2)}\right) - \dot{\epsilon}_1^{(1)}\dot{f}_0^{(2)}\right]\end{aligned} \tag{4.27}$$

Applying the integration rules 2.52 , 2.51 and 2.53 gives

$$
\begin{aligned}
\Sigma^{(2)}(\mu) &= \left(\frac{-\alpha_s L}{\pi}\right)^2 \left[\int_{Out}\frac{d\Omega_1}{4\pi}\int_{in}\frac{d\Omega_2}{4\pi}\epsilon_1^{(1)}\left(f_1^{(2)}-f_0^{(2)}\right) - \int_{In}\frac{d\Omega_1}{4\pi}\int_{In}\frac{d\Omega_2}{4\pi}\epsilon_1^{(1)}f_0^{(2)}\right] \\
&= \left(\frac{-\alpha_s L}{\pi}\right)^2 \left[\left(\int_c^1\frac{dx_1}{2}+\int_{-1}^{-c}\frac{dx_1}{2}\right)\int_0^{2\pi}\frac{d\phi_1}{2\pi}\Theta_{cut}\int_c^{-c}\frac{dx_2}{2}\int_0^{2\pi}\frac{d\phi_2}{2\pi}\Theta_{cut}\epsilon_1^{(1)}\left(f_1^{(2)}-f_0^{(2)}\right)\right. \\
&\left. - \int_c^{-c}\frac{dx_1}{2}\int_0^{2\pi}\frac{d\phi_1}{2\pi}\Theta_{cut}\int_{-c}^{c}\frac{dx_2}{2}\int_0^{2\pi}\frac{d\phi_2}{2\pi}\Theta_{cut}\epsilon_1^{(1)}f_0^{(2)}\right] \\
&= \left(\frac{-\alpha_s L}{\pi}\right)^2 \left[\left(\int_c^{1-\lambda}\frac{dx_1}{2}+\int_{\lambda-1}^{-c}\frac{dx_1}{2}\right)\int_c^{-c}\frac{dx_2}{2}\int_0^{2\pi}\frac{d\phi_2}{2\pi}\epsilon_1^{(1)}\left(f_1^{(2)}-f_0^{(2)}\right)\right. \\
&\left. - \int_c^{-c}\frac{dx_1}{2}\int_{-c}^{c}\frac{dx_2}{2}\int_0^{2\pi}\frac{d\phi_2}{2\pi}\epsilon_1^{(1)}f_0^{(2)}\right] \\
&= \left(\frac{-\alpha_s L}{\pi}\right)^2 \left[\left(\int_c^{1-\lambda}\frac{dx_1}{2}+\int_{\lambda-1}^{-c}\frac{dx_1}{2}\right)\int_c^{-c}\frac{dx_2}{2}\int_0^{2\pi}\frac{d\phi_2}{2\pi}\right. \\
&-2C_A C_F\omega_{ab}^1\frac{C_A}{2}\left(\omega_{a1}^2+\omega_{b1}^2-\omega_{ab}^2\right)\Theta_{cut} \\
&\left. - \int_c^{-c}\frac{dx_1}{2}\int_{-c}^{c}\frac{dx_2}{2}\int_0^{2\pi}\frac{d\phi_2}{2\pi}(-2C_A C_F\omega_{ab}^1 C_F\omega_{ab}^2)\Theta_{cut}\right] \\
&= \left(\frac{-\alpha_s L}{\pi}\right)^2 \left[-\left(\int_c^{1-\lambda}\frac{dx_1}{2}+\int_{\lambda-1}^{-c}\frac{dx_1}{2}\right)\int_{-c}^{c}\frac{dx_2}{2}\int_0^{2\pi}\frac{d\phi_2}{2\pi}\right. \\
&C_A^2 C_F\omega_{ab}^1\left(\omega_{a1}^2+\omega_{b1}^2-\omega_{ab}^2\right)\Theta(n_1\cdot n_2-\lambda) \\
&\left. + \int_0^c dx_1\int_0^c dx_2(2C_A C_F^2\omega_{ab}^1\omega_{ab}^2)\right]
\end{aligned}
\tag{4.28}
$$

where the Heaviside function (see equation 2.45) attached to the second term is redundant as the integral region does not include the poles at $n_1, n_2 \to n_a, n_b$. The integrand of the second term is also symmetric about $x_1 = 0$ and $x_2 = 0$ and has no azimuthal dependence. The first gluon is defined to travel along the $\phi_1 = 0$ direction meaning we can drop the first azimuthal dependence but this is not the case for ϕ_2 as

$$
\omega_{a1}^2 = \frac{n_a\cdot n_1}{n_a\cdot n_2 n_1\cdot n_2} = \frac{1-x_1}{(1-x_2)(1-y_1y_2\cos(\phi_2)-x_1x_2)} \tag{4.29}
$$

where $y_i = \sin(\theta_i)$. This term is also not symmetric about $x_1 = 0$ meaning the x_1 integral cannot be simplified.

Three poles remain at:

- $x_1 \to x_b = -1$
- $x_1 \to x_a = 1$

- $x_2 \to x_1 = c$ and $\phi_2 \to \phi_1 = 0$

The first two are not expected to diverge as the integrand vanishes at the pole. At the poles we have that

$$\omega_{a1}^2 + \omega_{b1}^2 - \omega_{ab}^2 \xrightarrow{n_1 \to n_a} \omega_{ba}^2 - \omega_{ab}^2 = 0 \tag{4.30}$$

and

$$\omega_{a1}^2 + \omega_{b1}^2 - \omega_{ab}^2 \xrightarrow{n_1 \to n_b} \omega_{ba}^2 - \omega_{ab}^2 = 0 \tag{4.31}$$

however this is just a heuristic approach and the numerics in the next chapter will demonstrate the cut-off independence.

The final pole occurs at the boundary of the jet opening angle where gluon one is in the out-of-gap region and gluon two is in the gap. The formal definition of the out of gap region is $x_1 < c$ rather than $x_1 \leq c$ so the pole is technically not reached. However, we would still expect a divergence leading up to the boundary and therefore a residual λ dependence.

4.7 Gaps between Jets up to third order

Using the results from the previous sections, up to third order the cross section is

$$
\begin{aligned}
\Sigma^{(3)}(\mu) &= \Sigma_0^{(3)}(\mu) + \Sigma_1^{(3)}(\mu) + \Sigma_2^{(3)}(\mu) + \Sigma_3^{(3)}(\mu) \\
&= \left(\frac{-\alpha_s L}{\pi}\right)^3 \left[\epsilon_0 \frac{\left(2\bar{f}_0^{(k)}\right)^3}{3!} + \frac{2}{3}\ddot{\epsilon}_1^{(1)}\left(\bar{f}_0^{(2)}\bar{f}_0^{(3)} + \bar{f}_1^{(2)}\bar{f}_0^{(3)} + \bar{f}_1^{(2)}\bar{f}_1^{(3)}\right)\right. \\
&\left. + \frac{\ddot{\epsilon}_2^{(1,2)}}{3}\left(\bar{f}_0^{(3)} + \bar{f}_1^{(3)} + \bar{f}_2^{(3)}\right) + \frac{1}{3\cdot 2}\ddot{\epsilon}_3^{(1,2,3)}\right] \\
&= \left(\frac{-\alpha_s L}{\pi}\right)^3 \left[-\left(-2\epsilon_0 \bar{f}_0^{(1)}\right)\frac{4}{3\cdot 2}\bar{f}_0^{(2)}\bar{f}_0^{(3)} + \frac{2}{3}\ddot{\epsilon}_1^{(1)}\bar{f}_0^{(2)}\bar{f}_0^{(3)} + \frac{2}{3}\ddot{\epsilon}_1^{(1)}\bar{f}_1^{(2)}\bar{f}_0^{(3)} + \frac{2}{3}\ddot{\epsilon}_1^{(1)}\bar{f}_1^{(2)}\bar{f}_1^{(3)}\right. \\
&\left. + \frac{1}{3}\left(-2\ddot{\epsilon}_1^{(1)}\ddot{f}_1^{(2)}\right)\bar{f}_0^{(3)} + \frac{1}{3}\left(-2\ddot{\epsilon}_1^{(1)}\ddot{f}_1^{(2)}\right)\bar{f}_1^{(3)} + \frac{1}{3}\ddot{\epsilon}_2^{(1,2)}\bar{f}_2^{(3)} + \frac{1}{3\cdot 2}\left(-2\ddot{\epsilon}_2^{(1,2)}\ddot{f}_2^{(3)}\right)\right] \\
&= \left(\frac{-\alpha_s L}{\pi}\right)^3 \left[\left(-\left(\bar{\epsilon}_1^{(1)}\right)\frac{2}{3}\bar{f}_0^{(2)}\bar{f}_0^{(3)} + \frac{2}{3}\ddot{\epsilon}_1^{(1)}\bar{f}_0^{(2)}\bar{f}_0^{(3)}\right) + \left(\frac{2}{3}\ddot{\epsilon}_1^{(1)}\bar{f}_1^{(2)}\bar{f}_0^{(3)} + \frac{1}{3}\left(-2\ddot{\epsilon}_1^{(1)}\ddot{f}_1^{(2)}\right)\bar{f}_0^{(3)}\right)\right. \\
&\left. + \left(\frac{2}{3}\ddot{\epsilon}_1^{(1)}\bar{f}_1^{(2)}\bar{f}_1^{(3)} + \frac{1}{3}\left(-2\ddot{\epsilon}_1^{(1)}\ddot{f}_1^{(2)}\right)\bar{f}_1^{(3)}\right) + \left(\frac{1}{3}\ddot{\epsilon}_2^{(1,2)}\bar{f}_2^{(3)} + \frac{1}{3\cdot 2}\left(-2\ddot{\epsilon}_2^{(1,2)}\ddot{f}_2^{(3)}\right)\right)\right] \\
&= \left(\frac{-\alpha_s L}{\pi}\right)^3 \left[-\frac{2}{3}\dot{\epsilon}_1^{(1)}\bar{f}_0^{(2)}\bar{f}_0^{(3)} + \frac{2}{3}\ddot{\epsilon}_1^{(1)}\dot{f}_1^{(2)}\bar{f}_0^{(3)} + \frac{2}{3}\ddot{\epsilon}_1^{(1)}\dot{f}_1^{(2)}\bar{f}_1^{(3)} - \frac{2}{3}\ddot{\epsilon}_1^{(1)}\ddot{f}_1^{(2)}\dot{f}_2^{(3)}\right] \\
&= \left(\frac{-\alpha_s L}{\pi}\right)^3 \frac{2}{3}\left[-\dot{\epsilon}_1^{(1)}\bar{f}_0^{(2)}\bar{f}_0^{(3)} + \ddot{\epsilon}_1^{(1)}\dot{f}_1^{(2)}\bar{f}_0^{(3)} + \ddot{\epsilon}_1^{(1)}\dot{f}_1^{(2)}\bar{f}_1^{(3)} - \ddot{\epsilon}_1^{(1)}\ddot{f}_1^{(2)}\dot{f}_2^{(3)}\right] \\
&= \left(\frac{-\alpha_s L}{\pi}\right)^3 \frac{2}{3}\left[-A + B + C - D\right]
\end{aligned}
\tag{4.32}
$$

where the $-D$ can be written as

$$
\begin{aligned}
-\frac{2}{3}\ddot{\epsilon}_1^{(1)}\ddot{f}_1^{(2)}\dot{f}_2^{(3)} = \frac{1}{3}\ddot{\epsilon}_2^{(1,2)}\dot{f}_2^{(3)} &= \int_{Out}\frac{d\Omega_1}{4\pi}\int_{Out}\frac{d\Omega_2}{4\pi}\int_{In}\frac{d\Omega_3}{4\pi}\frac{1}{3}\epsilon_2^{(1,2)}f_2^{(3)} \\
&= \int_{Out}\frac{d\Omega_1}{4\pi}\int_{Out}\frac{d\Omega_2}{4\pi}\int_{In}\frac{d\Omega_3}{4\pi}\frac{1}{3}\left(\frac{-1}{2}\epsilon_3^{(1,2,3)}\right).
\end{aligned}
\tag{4.33}
$$

The manipulations in equation 4.32 were carried out in an attempt to prove λ independence analytically and to greater understand the structure of the calculation in the hope of doing the same at higher orders. However, equation 4.32 does not present any clear arguments for λ independence. In the following chapter the final line is numerically integrated.

Chapter 5

Numerical Integration

5.1 Second Order

The numerical integration for $\Sigma^{(2)}$ was implemented easily in Mathematica and required only 5×10^5 sampling points for the in-built Monte-Carlo function to converge. I chose the following parameters to test the function:

- $\mu = 0.01$
- $Q = 1$
- $c = \frac{1}{\sqrt{2}} = \cos(\pi/4)$
- $\lambda = 10^{-1} \to 10^{-6}$

The results are shown in figure 5.1. As can be seen from figure 5.1 the observable is

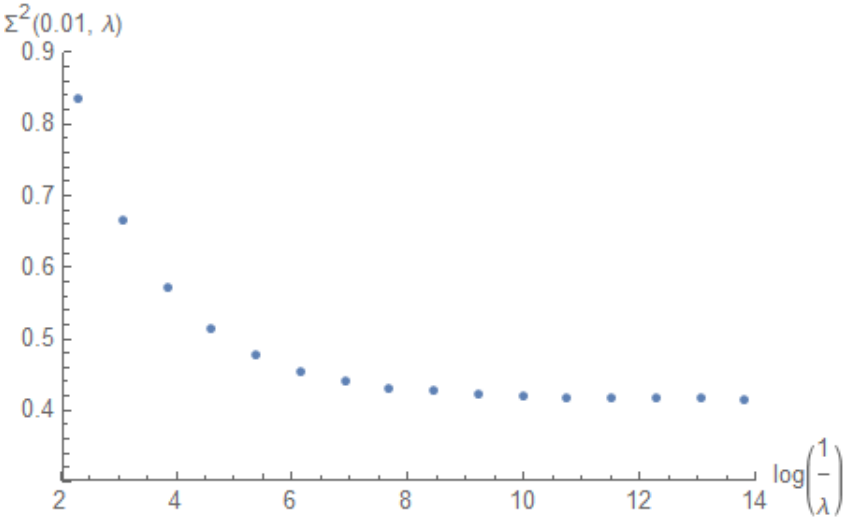

FIGURE 5.1: Dependence of $\Sigma^{(2)}$ on the Collinear Cut-off, λ.

independent of λ for

$$\begin{aligned} \ln(1/\lambda) &> 8 \\ \lambda &< 10^{-4} \end{aligned} \tag{5.1}$$

which is strong evidence that the co-linear divergences in $\Sigma^{(2)}$ cancel and the FKS algorithm works as it should. This suggests that the divergences at

- $x_1 \to x_b = -1$
- $x_1 \to x_a = 1$

cancel because the integrand vanishes as $n_1 \to n_a$ and $n_1 \to n_b$, as postulated in the previous chapter. The divergence at the pole

- $x_2 \to x_1 = c$ and $\phi_2 \to \phi_1 = 0$

clearly must also cancel. The reason for this cancellation is unclear, however. Further investigation into this type of cancellation would be helpful as this residual λ dependence at the boundary of the jet opening angle will occur at all orders. It occurs when a general emission function $f^{(k)}$ integrated over the out-of-gap region (real) is subtracted from the same emission function integrated over the entire phase space (virtual) which leaves

$$\bar{f}^{(k)} - \ddot{f}^{(k)} = \dot{f}^{(k)}. \tag{5.2}$$

As gluons are only emitted from real legs which by definition do not occur in the gap region, the gluon k can only be co-linear to the parent partons at the boundary of the two regions. This type of subtraction will occur most often for Bloch-Nordsieck type cancellations between terms with n reals and terms with $n-1$ reals and 1 virtual. For example,

$$2\ddot{\epsilon}_{n-1}^{(1\cdots n-1)}\bar{f}_{n-1}^{(n)} + \ddot{\epsilon}_{n}^{(1\cdots n)} = 2\ddot{\epsilon}_{n-1}^{(1\cdots n-1)}\bar{f}_{n-1}^{(n)} - 2\ddot{\epsilon}_{n-1}^{(1\cdots n-1)}\ddot{f}_{n-1}^{(n)} = 2\ddot{\epsilon}_{n-1}^{(1\cdots n-1)}\dot{f}_{n-1}^{(n)}. \tag{5.3}$$

But, as the manipulations of last chapter show, it could occur between less obviously paired terms. It would therefore be useful to understand whether the residual λ

dependence at the boundary will vanish for every subtraction of this form or whether it only works at second order.

The graph shows a strong dependence on λ as it approaches 1. This is expected as increasing λ corresponds to cutting increasingly large holes out of the phase space. Figure 5.1 suggests that the scale at which this effect becomes significant is $\lambda \approx 10^{-4}$.

5.2 Third Order

The numerical integration required for the third order calculation was more difficult. This is expected considering the integral contains many more singular regions. The in-built numerical integrator could not give a stable result and took too long to compute. I therefore used Suave, a numerical integrator from the Cuba package [22], which can handle highly oscillatory functions more effectively. I also expressed the integrands from A, B, C and D as piecewise functions which took the value of the integrand in the integration regions and zero elsewhere. The piecewise functions were then combined before being integrated over the entire phase space. This was to cancel as many divergences as possible prior to numerical integration rather than integrating over multiple divergent regions and summing the results. This helped to provide a stable result.

Another issue was the implementation of the Heaviside function, Θ_{cut}. The inbuilt *Heaviside* function gives a piecewise function which returns 0 if its argument is in the region to be cut from the phase space and unity otherwise. However, Mathematica simply then multiplies 0 with the attached function which is also evaluated. For example a radiation function appended with the cut-off function evaluates to

$$\begin{aligned} \omega_{ij}^{k}\Theta_{cut} &= \frac{n_i \cdot n_j}{n_i \cdot n_k n_k \cdot n_j}\Theta(n_i \cdot n_k - \lambda)\Theta(n_j \cdot n_k - \lambda) \\ &\xrightarrow{n_i \to n_k} \frac{1}{0} \times (0) \end{aligned} \tag{5.4}$$

if the singular point is sampled. Though the chances of this are low, with 20 poles in the phase space the effect is significant enough to cause the numerical integration to break down. Furthermore, as the number of points sampled increases, this becomes increasingly likely.

Instead of the inbuilt function I replaced every $\omega_{ij}^k \Theta_{cut}$ with an if statement

$$\text{If}[(n_i \cdot n_k > \lambda)\&\&(n_j \cdot n_k > \lambda), \omega_{ij}^k, 0] \tag{5.5}$$

which evaluates to the same piecewise function as the product of *Heaviside* functions but can also be integrated with other *Piecewise* functions. This rule was then applied to every radiation function in the A, B, C and D integrands. Applying *Piecewise-Expand* to the sum of each integrand then gave a single piecewise function which evaluated to zero if sampled within λ of any co-linear singularity or if in the vetoed region defined by the jet opening angle. In other words this method entirely cut the singular regions from the integral, as required. This was not a problem with $\Sigma^{(2)}$ because there were only three poles and the number of points required for the integral to converge was much lower.

The results for $\Sigma^{(3)}$ with $\lambda = 10^{-2} \to 10^{-6}$ using 10, 40 and 100 million points are shown in figure 5.2. Each plot used a different seed for the integration. The 10 million point plot diverges as $\lambda \to 0$ but with more points the graphs converge to the shape exhibited by the 100 million point plot. This plot displays λ independence in the region

$$\begin{aligned} \ln(1/\lambda) &< 11.5 \\ \lambda &< 10^{-5} \end{aligned} \tag{5.6}$$

and shows $\Sigma^{(3)}$ to vary by only 10% between $\lambda = 10^{-6} \to 10^{-3}$. Figure 5.3 displays each of the plots on the same axes. The lack of divergence as $\lambda \to 0$ for the observable at third order is evidence that the FKS algorithm is co-linear cut-off independent.

There are significant differences between the graphs for $\Sigma^{(3)}$ and the graph for $\Sigma^{(2)}$. First, the dependence on large λ is different for the two functions, the second order graph has a dependence close to $1/x$ for $\lambda > 10^{-4}$ and the third order graph displays a roughly logarithmic dependence $\ln(x)$ for $\lambda > 10^{-5}$ where x axis variable is $x = \ln\left(\frac{1}{\lambda}\right)$. The former positively diverges for large λ whereas the latter negatively diverges. As mentioned, the observable becomes meaningless for large λ as it corresponds to cutting significantly sized regions from the phase space, thus altering the requirements for the observable set using the measurement function. However, it would be beneficial

FIGURE 5.2: Dependence of $\Sigma^{(3)}$ on the Collinear Cut-off λ using 10, 40 and 100 million sampling points.

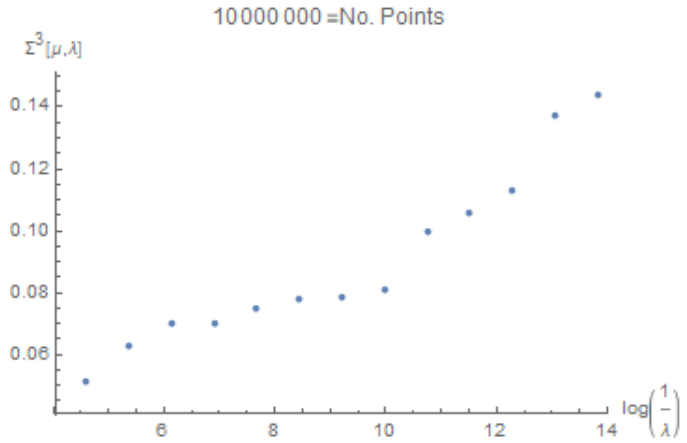

(a) The plot using 10 million points. This diverges as $\lambda \to 0$.

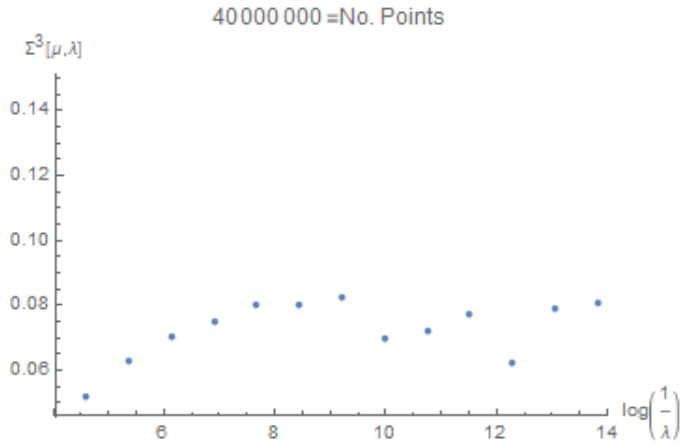

(b) The plot using 40 million points. The graph does not diverge as $\lambda \to 0$ but remains unstable for small λ.

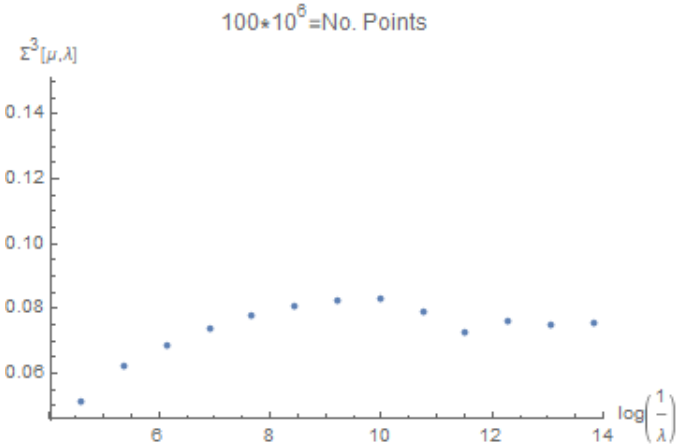

(c) The plot using 100 million points. The graph is λ independent for $\lambda < 10^{-5}$.

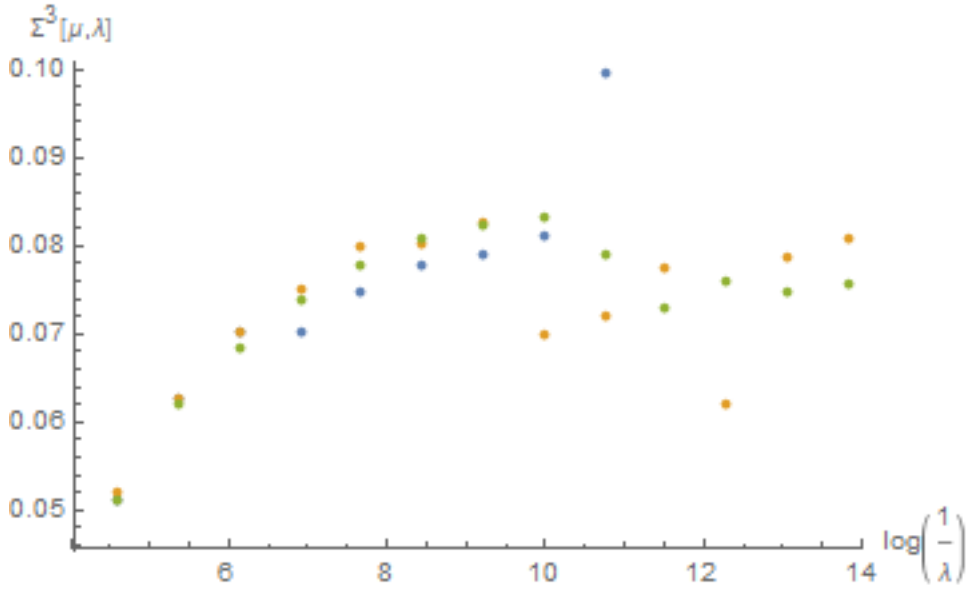

FIGURE 5.3: Dependence of $\Sigma^{(3)}$ on the Collinear Cut-off λ using 10, 40 and 100 million sampling points.

to understand why the two orders display distinct behaviours in these regions.

To summarize, these results suggest the algorithm does not depend on the collinear cut-off scale, suggesting collinear singularities cancel for the second and third order GBJ observable. Obvious topics for further study are higher order calculations, the same order using improved numerical techniques and investigations into the analytical cancellation of collinear poles. This was heuristically done for second order due to the small number of terms involved but the analytic proof proved intractable for the third order calculation. A route into these investigations could be to split the integral for third order and summing different combinations of integrated radiation functions. This would elucidate a possible cancellation regime that could in turn be applied to all orders.

Chapter 6

Conclusion

Soft gluon corrections provide logarithmic enhancements which cause the standard perturbative expansion of the Feynman rules to be invalid. Instead the perturbative series must be reordered, i.e. resummed, in terms of diagrams which are enhanced. For single soft gluon logarithms this amounts to a perturbative series in $\alpha_s \ln\left(\frac{Q}{\mu}\right)$. Fortunately, the Feynman rules in the soft approximation lead to the simplified eikonal rules. Non-global observables necessitate calculations involving real emissions. This greatly complicates the colour algebra. General parton shower event generators work in the large N limit to simplify these calculations but the approach was shown to omit vital super leading logarithms and so must be improved. The FKS algorithm derived these super leading logs and has since been developed to generate recursive QCD amplitudes for the radiation of any number of soft gluons and virtual corrections resummed to all orders. It is basis independent but the colour flow basis is a convenient choice. Using this basis the algorithm reproduced the BMS equation, a differential evolution equation for leading N resummations.

The algorithm is still in development and checks must be carried out on its validity. One such check is whether the observables it calculates are dependent on arbitrary parameters used to regularize singularities. If they are then the algorithm is producing invalid results. I consider the gaps between jets observable regularised from the collinear singularities using the collinear cut-off, λ. I used the algorithm to calculate the observable up to first, second and third order. I then explained how the colour flow basis is used to evaluate the colour structures in these calculations.

The first order expression was shown to be analytically λ independent. The second and third order expressions were evaluated numerically for a range of $\lambda = 10^{-2}$ to

$\lambda = 10^{-6}$ (the second order expression was evaluated down to $\lambda = 10^{-1}$). For second order the observable was independent of λ in the region $\lambda < 10^{-4}$. For λ above this scale the observable positively diverged for increasing λ, though the exact dependence was not tested.

The observable for third order required $\mathcal{O}(1000)$ more points to produce a plot which was numerically stable. The final plot gave λ independence in the region $\lambda < 10^{-5}$. The dependence above this scale was negatively divergent for increasing λ.

In both cases the collinear singularities have been shown to cancel and this is a success of the algorithm. However, the structure of these cancellations is unclear. Further work would attempt to identify these structures in a hope to find an analytic proof for λ independence of the algorithm at all orders.

Bibliography

[1] R. Keith Ellis, W. James Stirling, and B. R. Webber. "QCD and collider physics". In: *Camb. Monogr. Part. Phys. Nucl. Phys. Cosmol.* 8 (1996), pp. 1–435.

[2] Michael E. Peskin and Daniel V. Schroeder. *An Introduction to quantum field theory*. Reading, USA: Addison-Wesley, 1995. ISBN: 9780201503975, 0201503972. URL: http://www.slac.stanford.edu/~mpeskin/QFT.html.

[3] F. Halzen and Alan D. Martin. *QUARKS AND LEPTONS: AN INTRODUCTORY COURSE IN MODERN PARTICLE PHYSICS*. 1984. ISBN: 0471887412, 9780471887416.

[4] Stefan Höche. "Introduction to parton-shower event generators". In: *Proceedings, Theoretical Advanced Study Institute in Elementary Particle Physics: Journeys Through the Precision Frontier: Amplitudes for Colliders (TASI 2014): Boulder, Colorado, June 2-27, 2014*. 2015, pp. 235–295. DOI: 10.1142/9789814678766_0005. arXiv: 1411.4085 [hep-ph].

[5] Rene Angeles Martinez. "Coulomb gluons and the ordering variable". PhD thesis. Manchester,UK: The University of Manchester, 2016.

[6] Andy Buckley et al. "General-purpose event generators for LHC physics". In: *Phys. Rept.* 504 (2011), pp. 145–233. DOI: 10.1016/j.physrep.2011.03.005. arXiv: 1101.2599 [hep-ph].

[7] S. Catani. "Soft gluon resummation: A Short review". In: *QCD and high energy hadronic interactions. Proceedings, 32nd Rencontres de Moriond, Les Arcs, France, March 22-29, 1997*. 1997, pp. 331–336. arXiv: hep-ph/9709503 [hep-ph].

[8] Eric Laenen, Gianluca Oderda, and George Sterman. "Resummation of threshold corrections for single-particle inclusive cross sections". In: *Physics Letters B* 438.1-2 (Oct. 1998), pp. 173–183. ISSN: 0370-2693. DOI: 10.1016/s0370-

2693(98)00960-5. URL: http://dx.doi.org/10.1016/S0370-2693(98)00960-5.

[9] F. Bloch and A. Nordsieck. "Note on the Radiation Field of the electron". In: *Phys. Rev.* 52 (1937), pp. 54–59. DOI: 10.1103/PhysRev.52.54.

[10] René Ángeles Martínez et al. "Soft gluon evolution and non-global logarithms". In: *JHEP* 05 (2018), p. 044. DOI: 10.1007/JHEP05(2018)044. arXiv: 1802.08531 [hep-ph].

[11] M. Dasgupta and G.P. Salam. "Resummation of non-global QCD observables". In: *Physics Letters B* 512.3-4 (July 2001), pp. 323–330. ISSN: 0370-2693. DOI: 10.1016/s0370-2693(01)00725-0. URL: http://dx.doi.org/10.1016/S0370-2693(01)00725-0.

[12] Gerard 't Hooft. "A Planar Diagram Theory for Strong Interactions". In: *Nucl. Phys.* B72 (1974). [,337(1973)], p. 461. DOI: 10.1016/0550-3213(74)90154-0.

[13] Manuel Bähr et al. "Herwig++ physics and manual". In: *The European Physical Journal C* 58.4 (Nov. 2008), pp. 639–707. ISSN: 1434-6052. DOI: 10.1140/epjc/s10052-008-0798-9. URL: http://dx.doi.org/10.1140/epjc/s10052-008-0798-9.

[14] Torbjörn Sjöstrand et al. "An introduction to PYTHIA 8.2". In: *Computer Physics Communications* 191 (June 2015), pp. 159–177. ISSN: 0010-4655. DOI: 10.1016/j.cpc.2015.01.024. URL: http://dx.doi.org/10.1016/j.cpc.2015.01.024.

[15] T. Gleisberg et al. "Event generation with SHERPA 1.1". In: 2009.

[16] Jeffrey R Forshaw, Albrecht Kyrieleis, and Michael H Seymour. "Super-leading logarithms in non-global observables in QCD?" In: *Journal of High Energy Physics* 2006.08 (Aug. 2006), pp. 059–059. ISSN: 1029-8479. DOI: 10.1088/1126-6708/2006/08/059. URL: http://dx.doi.org/10.1088/1126-6708/2006/08/059.

[17] J.R Forshaw, A Kyrieleis, and M.H Seymour. "Super-leading logarithms in non-global observables in QCD: colour basis independent calculation". In: *Journal of High Energy Physics* 2008.09 (Sept. 2008), pp. 128–128. ISSN: 1029-8479. DOI:

10.1088/1126-6708/2008/09/128. URL: http://dx.doi.org/10.1088/1126-6708/2008/09/128.

[18] Jeffrey R. Forshaw, Michael H. Seymour, and Andrzej Siódmok. "On the breaking of collinear factorization in QCD". In: *Journal of High Energy Physics* 2012 (2012), pp. 1–16.

[19] Andrea Banfi, Giuseppe Marchesini, and Graham Smye. "Away-from-jet energy flow". In: *Journal of High Energy Physics* 2002.08 (Aug. 2002), pp. 006–006. ISSN: 1029-8479. DOI: 10.1088/1126-6708/2002/08/006. URL: http://dx.doi.org/10.1088/1126-6708/2002/08/006.

[20] F. Maltoni et al. "Color-flow decomposition of QCD amplitudes". In: *Physical Review D* 67.1 (Jan. 2003). ISSN: 1089-4918. DOI: 10.1103/physrevd.67.014026. URL: http://dx.doi.org/10.1103/PhysRevD.67.014026.

[21] M. Yates. "Understanding Gluon Radiation In Interjet Regions". MA thesis. The University of Manchester (United Kingdom, 2010.

[22] Thomas Hahn. "Cuba - a library for multidimensional numerical integration". In: *Computer Physics Communications* 168 (2005), pp. 78–95.